Chapter 5

Fault-tolerant control

5.1 Introduction

In the existing papers on train handling as well as the previous chapters, all the controllers are designed on the assumption that the train is well set up and all the actuators (traction efforts and braking efforts of locomotives and wagons) and sensors (speed sensors) work as designed, which is an ideal condition. In practice, some of the actuators and/or sensors may be faulty, and even worse, the train structure may be changed. For example, the speed sensor has a constant bias, or the amplifier in the sensor circuit has a fault, which leads to a gain fault of the sensor. The air pressure in the braking pipe may be different from expected because of a fault in the pressure sensor in the air recharge system or air leakage, which makes the braking forces acting on the wheels less than expected. When a fault happens, the controller, designed on the basis of the faultless train model, cannot work as well as expected, and sometimes it even leads to unsafe running, such as train-breaking and derailment, *i.e.,* the safe running of trains cannot be promised. Some safe running methods are therefore necessary in train handling.

Actually, in some fault modes of train handling, it is possible to assure train performance with suitably redesigned controllers. That is what is studied in this chapter.

In nature, the above-mentioned controller redesign is a fault-tolerant control problem. In the literature, there are many papers about such problems. Some survey papers, such as [48, 49, 50, 51, 52, 53, 54, 55], provide excellent reviews on the subject of fault-tolerant control. For linear systems, geometric approaches are proposed for fault detection and isolation (FDI), e.g. in [56, 57, 58]. A combined input-output and local approach is proposed in [59] for the problem of FDI of nonlinear systems modelled by polynomial differential-algebraic equations. A high-gain observer-based approach for FDI of an affine nonlinear system is advanced in [60], where a sufficient condition is

given. In [61], a geometric approach to FDI of nonlinear systems is proposed, while a necessary condition for the existence of FDI is exploited based on a geometric concept– *unobservability distribution* introduced by the authors in [62]. For the solution of FDI, a sufficient condition is also given. A stability- and performance-vulnerable failure of sensors can be identified with the approach in [63] for nonlinear systems. The switch between two robust control strategies based on normal operation and faulty operation is used to realize fault-tolerant control. An information-based diagnostic approach is investigated in [64] for a class of SISO nonlinear system in a triangular structure. In [65], a fault diagnosis approach is proposed based on adaptive estimation by combining a high gain observer and a linear adaptive observer. As is known, the high-gain observer is sensitive to measurement noise. In speed regulation of heavy haul trains with measurement (speeds) feedback, noise is inevitable, so a high-gain observer is not considered in this study. Recently, compared to [61], a relaxed formulation of FDI of nonlinear systems is proposed in [66], where a residual has been designed to detect a set of faults.

In train handling, such problems have been investigated in [69, 70] for some faults with induction motors. The fault detection and isolation of diesel engines are seen in [67, 68]. Paper [70] is in essence on fault-tolerant control of the induction motor, which can also be seen in [71]. In this chapter, the fault-tolerant control of the whole train is studied. The faulty modes of a train include the gain faults of speed sensors, the locomotive actuators (induction motors, in this study), and wagon actuators (the braking systems). The locomotive fault signal is assumed to be acquired from other FDIs and is available in its fault-tolerant controller redesign. Based on the train model and fault modes, a fault-tolerant speed regulator (including the FDI part and FTC part) is designed for the faults of sensors and braking systems, respectively. The fault-tolerant speed regulator of sensors' faults is based on the approach in [61], while the fault-tolerant speed regulator of the braking system fault is based on steady state calculation.

In this chapter, a geometric approach to fault detectability is quoted from [61] in section 5.2. The approach in [61] is employed for the FDI of sensor faults. Then the fault modes of train handling are assumed with sensor faults and actuator faults, respectively. Considering the convenience of application considered, the sensor equipment structure of a train is suggested and the train structure is assumed for the subsequent study. The third part, the application condition of the result in section 5.2, is justified for the speed sensors as well as for the wagon actuators. An FDI for the sensor faults is designed on the basis of the approach in [61] and an FDI for the wagon actuator faults is designed on the basis of an approach proposed in this thesis. Based on the fault signals, the fault-tolerant controller is very convenient to be redesigned. Simulation for the proposed approaches is also given in the last part of this chapter.

5.2 Fault detectability

Based on a concept of the *observability co-distribution* in [62], a geometric approach is proposed in [61] for the fault detection problem of nonlinear systems. This approach will be adopted to justify the detectability of the train faults.

Consider a nonlinear system in the following form,

$$\begin{aligned} \dot{x} &= f(x) + g(x)u + l(x)u_f + p(x)w, \\ y &= h(x), \end{aligned} \tag{5.1}$$

where $x \in X \subset R^n$ is the state with X a neighbourhood of the origin, $u \in R^{m_u}$ is the control input, $u_f \in R$ is a fault signal (input), $w \in R^d$ is the disturbance and/or other fault signals, and $y \in R^q$ is the output. $g(x) = [g_1(x), \cdots, g_{m_u}(x)]$ and it is assumed $g_0(x) = f(x)$. $p(x) = [p_1(x), \cdots, p_d(x)]$. The vector fields $g_i(x), i \in [0, m_u], p_j(x), j \in [1, d], h(x)$ are assumed to be smooth and $f(0) = 0, h(0) = 0$.

The task of fault detection is to design a filter (*residual generator*) in the form of

$$\begin{aligned} \dot{\hat{x}} &= \hat{f}(\hat{x}, y) + \hat{g}(\hat{x}, y)u, \\ r &= \hat{h}(\hat{x}, y), \end{aligned} \tag{5.2}$$

where $\hat{x} \in \hat{X} \subset R^{\hat{n}}$, $r \in R^{\hat{q}}, \hat{q} \leq q$, and the vector fields $\hat{f}(\hat{x}, y), \hat{g}(\hat{x}, y), \hat{h}(\hat{x}, y)$ are smooth and $\hat{f}(0, 0) = 0, \hat{h}(0, 0) = 0$ such that the output r of the cascade system composed of (5.1) and (5.2) depends only on the fault signal u_f, is decoupled from the disturbance w and asymptotically converges to zero whenever u_f is identically zero with any input u.

This problem is formulated in a geometric concept in [61].

The system (5.1) can be rewritten as follows without the fault and disturbance signals considered:

$$\begin{aligned} \dot{x} &= g_0(x) + \sum_{i=1}^{m_u} g_i(x)u_i, \\ y &= h(x). \end{aligned} \tag{5.3}$$

Based on this system, some concepts are given below.

$\ker\{dh\}$ is the distribution annihilating the differentials of the rows of the mapping $h(x)$.

$\text{span}\{dh\}$ is the co-distribution spanned by the differentials of the rows of the mapping $h(x)$.

A distribution Δ is said to be conditioned invariant ((h, f) invariant, $f = g_0$) of the

system (5.3) if it satisfies

$$[g_i, \Delta \cap \ker\{dh\}] \subset \Delta, \forall i \in [0, m_u], \tag{5.4}$$

A co-distribution Ω is said to be conditioned invariant if

$$L_{g_i}\Omega \subset \Omega + \text{span}\{dh\}, \forall i \in [0, m_u]. \tag{5.5}$$

The symbol Ω_o denotes the smallest co-distribution invariant under $g_i, i \in [0, m_u]$ which contains $\text{span}\{dh\}$.

The cascade system of (5.1) and (5.2) can be written as

$$\begin{aligned} \dot{x}^e &= g_0^e(x^e) + \sum_{i=1}^{m_u} g_i^e(x^e)u_i + l^e(x^e)u_f + \sum_{i=1}^{d} p_i^e(x^e)w_i, \\ r &= h^e(x^e), \end{aligned} \tag{5.6}$$

where $x^e = \begin{pmatrix} x \\ \hat{x} \end{pmatrix}$, $g_0^e(x^e) = \begin{pmatrix} f(x) \\ \hat{f}(\hat{x}, h(x)) \end{pmatrix}$, $g_i^e(x^e) = \begin{pmatrix} g_i(x) \\ \hat{g}_i(\hat{x}, h(x)) \end{pmatrix}, i \in [1, m_u]$,
$l^e(x^e) = \begin{pmatrix} l(x) \\ 0 \end{pmatrix}$, $p_i^e(x^e) = \begin{pmatrix} p_i(x) \\ 0 \end{pmatrix}, i \in [1, d]$,

$h^e(x^e) = \hat{h}(\hat{x}, h(x))$. Let Ω_o^e denote the smallest co-distribution invariant under $g_i^e, i \in [0, m]$ which contains $\text{span}\{dh^e\}$.

The local nonlinear fundamental problem of residual generation (lNLFPRG) can be formulated in a geometric way [61].

Problem: Given a system (5.1)*, find, if possible, a dynamic system in the form of* (5.2) *such that the smallest co-distribution invariant* Ω_o^e *defined in* (5.6) *satisfies*

i) $\text{span}\{p_1^e, \cdots, p_d^e\} \subset (\Omega_o^e)^\perp$;

ii) $\text{span}\{l^e\} \not\subset (\Omega_o^e)^\perp$;

iii) there exists a neighbourhood of $X^e \in R^{n+\hat{n}}$ *containing the origin, such that the output* r *of system* (5.6) *asymptotically converges to zeros when* $u_f(t) = 0$ *and* $x^e(0) \in X^e$.

The fault detectability of nonlinear systems is incorporated with the *conditioned invariant distribution* and *observability co-distribution* [61].

An algorithm is given in [61] for a conditioned invariant distribution for the system (5.3) as follows. The nondecreasing sequence of distributions is defined:

$$\begin{aligned} S_0 &= \bar{P}, \\ S_{k+1} &= \bar{S}_k + \sum_{i=0}^{m_u} [g_i, \bar{S}_k \cap \ker\{dh\}], \end{aligned} \tag{5.7}$$

where $P = \text{span}\{p_1(x), \cdots, p_d(x)\}$ and $\bar{S}$ denotes the involutive closure of S. Then the following lemma holds.

Lemma. Suppose there exists an integer k^* such that

$$S_{k^*+1} = \bar{S}_{k^*}, \tag{5.8}$$

and set $\Sigma_*^P = \bar{S}_{k^*}$. Then Σ_*^P is involutive, contains P and is the smallest conditioned invariant.

One can see that $(\Sigma_*^P)^\perp$ is the maximal conditioned invariant co-distribution, which is locally spanned by exact differentials and contained in $P^\perp$.

An algorithm is also given for an observability co-distribution of the system (5.3). Let Θ be a fixed co-distribution and define the following nondecreasing sequence of co-distributions

$$\begin{aligned} Q_0 &= \Theta \cap \text{span}\{dh\}, \\ Q_{k+1} &= \Theta \cap \left(\sum_{i=0}^{m_u} L_{g_i} Q_k + \text{span}\{dh\} \right). \end{aligned} \tag{5.9}$$

Suppose that all co-distributions of this sequence are nonsingular, so that there exists an integer $k^* \leq n-1$ such that $Q_k = Q_{k^*}, \forall k > k^*$, and set $\Omega^* = \Omega_{k^*} = o.c.a(\Theta)$, where "o.c.a" stands for "observability co-distribution algorithm". Then the following holds.

Proposition. Suppose all the co-distributions generated by the algorithm above are nonsingular. Then repeat the algorithm above with $\Theta' = o.c.a(\Theta)$, that is,

$$\begin{aligned} Q_0 &= \Omega^* \cap span\{dh\}, \\ Q_{k+1} &= \Omega^* \cap \left(\sum_{i=0}^{m_u} L_{g_i} Q_k + span\{dh\} \right). \end{aligned} \tag{5.10}$$

As a consequence, $\Omega^* = o.c.a(\Omega^*)$. If the co-distribution Θ is conditioned invariant, so is Ω^*.

A co-distribution Ω is said to be an observability co-distribution for the system (5.3) if

$$\begin{aligned} &L_{g_i}\Omega \subset \Omega + \text{span}\{dh\}, \forall i \in [0, m_u], \\ &o.c.a(\Omega) = \Omega. \end{aligned} \tag{5.11}$$

A distribution Δ is an unobservability distribution if its annihilator $\Omega = (\Delta)^{\perp}$ is an observability co-distribution.

Also it is true that the co-distribution $o.c.a(\Theta)$ is the maximal observability co-distribution contained in Θ. If the distribution Σ_*^P is well-defined and nonsingular, and $\Sigma_*^P \cap \ker\{dh\}$ is a smooth co-distribution, then
$o.c.a((\Sigma_*^P)^{\perp})$ is the maximal observability co-distribution, which is locally spanned by exact differentials and contained in $P^{\perp}$.

A necessary condition for the solvability of lNLFPRG is that

$$\text{span}\{l\} \not\subset \left(o.c.a(\Sigma_*^P)^{\perp})\right)^{\perp}. \tag{5.12}$$

A sufficient condition is also given in [61].

Consider a system (5.1), determine the co-distribution $o.c.a(\Sigma_*^P)^{\perp})$, the largest observability co-distribution locally spanned by exact differentials and contained in $P^{\perp}$, and suppose the necessary condition (5.12) is satisfied. Then the system (5.1) can be rewritten as follows

$$\begin{aligned}
\dot{z}_1 &= f_1(z_1, z_2) + g_1(z_1, z_2)u + l_1(z_1, z_2, z_3)u_f, \\
\dot{z}_2 &= f_2(z_1, z_2, z_3) + g_2(z_1, z_2, z_3)u, \\
\dot{z}_3 &= f_3(z_1, z_2, z_3) + g_3(z_1, z_2, z_3)u, \\
y_1 &= h_1(z_1), \\
y_2 &= z_2,
\end{aligned} \tag{5.13}$$

with a coordinate change

$$z = \Phi(x) = \begin{pmatrix} z_1 \\ z_2 \\ z_3 \end{pmatrix} = \begin{pmatrix} \Phi_1(x) \\ H_2 h(x) \\ \Phi_3(x) \end{pmatrix}, \tag{5.14}$$

where $\Phi(x)$ is determined as described below.

When the fault signal and the disturbance signals are not considered, the system (5.1) is the one (5.3). Consider this system, let Ω be an observability co-distribution and $n_1 = \dim(\Omega)$. Suppose Ω is spanned by exact differentials and $\text{span}\{dh\}$ is nonsingular. $q - n_2 = \dim(\Omega \cap \text{span}\{dh\})$. Suppose there exists a surjection $\Psi_1 : R^p \to R^{p-n_2}$ such that

$$\Omega \cap \text{span}\{dh\} = \text{span}\{d(\Psi_1 \circ h)\}.$$

At $x^o \in X$, a neighourhood of the origin ($y^o = h(x^o)$), there exists a selection matrix H_2 (*i.e.,* a matrix in which any row has all zero entries but one, which is equal to one) such that

$$\Psi(y) = \begin{pmatrix} y_1 \\ y_2 \end{pmatrix} = \begin{pmatrix} \Psi_1(y) \\ H_2 y \end{pmatrix} \tag{5.15}$$

is a local diffeomorphism at $y^o \in R^p$. Choose a function $\Phi_1 : U^o \to R^{n_1}$, where U^o is a neighbourhood of x^o, such that in U^o,

$$\Omega = \text{span}\{d\Phi_1\}.$$

Then there exists a function $\Phi_3 : U^o \to R^{n-n_1-n_2}$ such that $\Phi(x)$ in (5.14) is a local diffeomorphism at $x^o \in U^o$. With this coordinate change, the system (5.3) is described in the following form,

$$\begin{aligned}
\dot{z}_1 &= f_1(z_1, z_2) + g_1(z_1, z_2)u \\
\dot{z}_2 &= f_2(z_1, z_2, z_3) + g_2(z_1, z_2, z_3)u, \\
\dot{z}_3 &= f_3(z_1, z_2, z_3) + g_3(z_1, z_2, z_3)u, \\
y_1 &= h_1(z_1), \\
y_2 &= z_2.
\end{aligned} \tag{5.16}$$

If $p(x)$ is a vector field in the annihilator of Ω, (which is true when $\Omega \subseteq \Sigma_*^P$,) and the condition (5.12) is satisfied, then in the new coordinates, the system (5.1) is in the form

$$\begin{aligned}
\dot{z}_1 &= f_1(z_1, z_2) + g_1(z_1, z_2)u + l_1(z_1, z_2, z_3)u_f, \\
\dot{z}_2 &= f_2(z_1, z_2, z_3) + g_2(z_1, z_2, z_3)u + l_2(z_1, z_2, z_3)u_f + p_2(z_1, z_2, z_3)w, \\
\dot{z}_3 &= f_3(z_1, z_2, z_3) + g_3(z_1, z_2, z_3)u + l_3(z_1, z_2, z_3)u_f + p_3(z_1, z_2, z_3)w, \\
y_1 &= h_1(z_1), \\
y_2 &= z_2.
\end{aligned} \tag{5.17}$$

It is very interesting to study the following z_1-system of (5.16), which is *locally weakly observable* with inputs u, y_1, and y_2 if $g_1(z_1, z_2)$ is a sum of a vector field of z_1 and a vector field of z_2.

$$\begin{aligned}
\dot{z}_1 &= f_1(z_1, y_2) + g_1(z_1, y_2)u, \\
y_1 &= h_1(z_1).
\end{aligned} \tag{5.18}$$

The following system is also locally weakly observable,

$$\begin{aligned}
\dot{z}_1 &= f_1(z_1, y_2) + g_1(z_1, y_2)u + l_1(z_1, z_2, z_3)u_f, \\
y_1 &= h_1(z_1).
\end{aligned} \tag{5.19}$$

As assumed in (5.12), $l_1(z_1, z_2, z_3)$ is non-zero. So the occurrence of the fault signal u_f may be detected by an appropriate observer.

5.3 Fault modes of trains

The previous train model is repeated as follows,

$$\begin{aligned}
m_i\dot{v}_i &= u_i + f_{in_{i-1}} - f_{in_i} - f_{a_i}, \qquad i = 1, \cdots, n, \\
\dot{x}_j &= v_j - v_{j+1}, \qquad j = 1, \cdots, n-1.
\end{aligned} \tag{5.20}$$

With open loop scheduling, one can get the equilibria. Then a difference system between the train model and the equilibria is as (3.21), which can be rewritten as

$$\begin{aligned} \delta\dot{v} &= f_{11}(\delta v) + A_{12}\delta x + B\delta u, \\ \delta\dot{x} &= A_{21}\delta v. \end{aligned} \tag{5.21}$$

where $\delta v = col(\delta v_1, \ ..., \delta v_n)$, $\delta x = col(\delta x_1, \ ..., \delta x_{n-1})$, $f_{11}(\delta v) = [f_{11}^1(\delta v_1), \ ..., f_{11}^n(\delta v_n)]^T$ in which $f_{11}^i(\delta v_i) = (c_{1_i} + 2c_{2_i}v_r)\delta v_i + c_{2_i}\delta v_i^2$,

$$B = \text{diag}(\frac{1}{m_1}, \cdots, \frac{1}{m_n}),$$

$$A_{12} = \begin{bmatrix} -\frac{k_1}{m_1} & 0 & \cdots & 0 & 0 \\ \frac{k_1}{m_2} & -\frac{k_2}{m_2} & \cdots & 0 & 0 \\ \cdots & \cdots & \cdots & \cdots & \cdots \\ 0 & \cdots & 0 & \frac{k_{n-2}}{m_{n-1}} & -\frac{k_{n-1}}{m_{n-1}} \\ 0 & \cdots & 0 & 0 & \frac{k_{n-1}}{m_n} \end{bmatrix},$$

$$A_{21} = \begin{bmatrix} 1 & -1 & 0 & \cdots & 0 & 0 \\ 0 & 1 & -1 & \cdots & 0 & 0 \\ \cdots & \cdots & \cdots & \cdots & \cdots & \cdots \\ 0 & 0 & 0 & \cdots & 1 & -1 \end{bmatrix}.$$

The variables $k_i, \ i = 1, \cdots, n-1$ are chosen to be constant.

In this thesis, the fault modes include speed senor faults and actuator faults.

5.3.1 Speed sensor faults

The states of a train include the speeds of cars and the relative displacement of the couplers (in-train forces). It is practical to measure the speeds of cars. The speed sensor may be faulty with a constant bias, and/or with a gain fault due to the gain change of the amplifier in the circuit. In the former case, such a fault can be corrected by the calibration before its application. In this chapter, the latter case is considered, that is, the sensor for the ith car's speed is faulty with a gain fault,

$$v_i = (1 + m_{v_i}^f)v_i^o, \tag{5.22}$$

where the variable v_i is the sensor output for the ith car's speed, v_i^o is the real speed, and $m_{v_i}^f$ is the constant gain fault of the sensor.

Assuming there are q sensors equipped for q cars of the train, and they are located at the positions $ls_1, \cdots, ls_q$, then, the dynamics of a train with speed measurement

(5.21) is as follows,

$$\begin{aligned} \delta\dot{v} &= f_{11}(\delta v) + A_{12}\delta x + Bu, \\ \delta\dot{x} &= A_{21}\delta v, \\ y_i &= (1 + m^f_{v_{ls_i}})v_{ls_i} - v_r, \qquad i = 1, \cdots, q, \end{aligned} \tag{5.23}$$

where the variable $m^f_{v_{ls_i}}$ is the constant gain fault of the ith sensor.

5.3.2 Actuator faults

The actuators of a train include the locomotives' engines (traction efforts or dynamic braking forces) and the wagons' brakes (braking efforts). However, the actuators are sometimes faulty. For example, one locomotive in a locomotive group (composed of n_l locomotives) does not work, then the actual output of the locomotive group is $\frac{n_l-1}{n_l}$ of the expected. The air pressure in the braking pipe is sometimes different from the designed one owing to air leakage or a fault of the pressure sensor in the air recharging system, which leads to less braking effort in the braking system. In train handling, every locomotive has its own engine, whose running condition is independent with the others while all wagons share the same braking pressure in the air pipe along the train, whose fault leads to the same faults on all wagons.

In the above cases, the outputs of the actuators may not be equal to those expected, but proportional to the expected ones, *i.e.,*

$$u^f_i = (1 - m^i_f)u_i, \qquad i = 1, \cdots, n, \tag{5.24}$$

in which u_i, u^f_i are expected output and real output, respectively. The output includes the open loop part u^o_i and the closed-loop part U_i. The coefficient m^i_f is a fault coefficient. In (5.24), $0 \leq m^i_f \leq 1$.

In the following analysis, one assumes the locomotives' faults are independent and the wagons' faults are the same, *i.e.,*

$$\begin{aligned} u^f_{l_i} &= (1 - m^{l_i}_f)u_{l_i}, \quad i = 1, \cdots, k, \\ u^f_j &= (1 - m^w_f)u_j, \quad j = 1, \cdots, n, j \neq l_i. \end{aligned} \tag{5.25}$$

5.4 Fault detection and isolation

5.4.1 Sensor fault detection and isolation

The sensors in train handling are the speed sensors. When the faults of these sensors are considered and viewed as pseudo-actuators' faults, the train model described in

(5.23), is as follows.

$$\begin{aligned}
\delta\dot{v} &= f_{11}(\delta v) + A_{12}\delta x + BU,\\
\delta\dot{x} &= A_{21}\delta v,\\
\dot{v}^f_{ls_i} &= -v^f_{ls_i} + u^f_{ls_i} v_{ls_i},\\
y_i &= \delta v_{ls_i} + v^f_{ls_i}, \qquad i = 1, \cdots, q,
\end{aligned} \tag{5.26}$$

where $u^f_{ls_i}$ is the pseudo-actuator of the sensor fault. When there is no fault with the sensor, *i.e.*, $v^f_{ls_i} = 0$, the dynamics are $\dot{v}^f_{ls_i} = -v^f_{ls_i} + u^f_{ls_i} v_{ls_i}$, in which $u^f_{ls_i}$ must be zero. When there is a fault with the sensor, *i.e.*, $v^f_{ls_i} \neq 0$, one has $u^f_{ls_i} = \frac{v^f_{ls_i}}{v_{ls_i}} \neq 0$ in steady state. So $u^f_{ls_i}$ can be thought of as the sensor fault signal.

In the previous chapter, it is assumed that there is a speed sensor for the first car (usually a locomotive). It is convenient to assume that this sensor is always in good condition and the output of this sensor is y_1, which can be guaranteed by some hardware structures, for example, a hardware redundancy. With this assumption, for every sensor fault mode (the output of this sensor is $y_i, i = 2, \cdots, q$), the train is modelled as

$$\begin{aligned}
\delta\dot{v} &= f_{11}(\delta v) + A_{12}\delta x + BU,\\
\delta\dot{x} &= A_{21}\delta v,\\
\dot{v}^f_{ls_i} &= -v^f_{ls_i} + u^f_{ls_i} v_{ls_i},\\
y_1 &= \delta v_1,\\
y_i &= \delta v_{ls_i} + v^f_{ls_i}, \qquad i = 2, \cdots, q.
\end{aligned} \tag{5.27}$$

When the ith sensor fault $u^f_{ls_i}$ is considered as u_f in (5.1), the other sensor faults ($u^f_{ls_j},\ j \in [2, q],\ j \neq i$) are thought as w in (5.1) to be decoupled. Then in the form of (5.1), one has $x = [\delta v, \delta x, v^f_{ls}]^T$, $u = U$, $u_f = u^f_{ls_i}$, $w = (u^f_{ls_j}), j \in [2, q], j \neq i$,

$$f(x) = \begin{bmatrix} f_{11}(\delta v) + A_{12}\delta x \\ A_{21}\delta v \end{bmatrix},$$

$$g(x) = B,$$

$$l(x) = [\overbrace{0, \cdots, 0}^{n-2+i}, v_{ls_i}, \overbrace{0, \cdots, 0}^{q-i}]^T,$$

$$p_j(x) = [\overbrace{0, \cdots, 0}^{n-2+j}, v_{ls_j}, \overbrace{0, \cdots, 0}^{q-j}]^T, j \in [2, q], j \neq i,$$

and

$$h(x) = \begin{bmatrix} \delta v_1 \\ \delta v_{ls_2} \\ \cdots \\ \delta v_{ls_q} \end{bmatrix}.$$

For the system (5.27), assuming the co-distribution

$$\Theta = \Omega_0 = \text{span}\{d(\delta v_1), \cdots, d(\delta v_n), d(\delta x_1), d(\delta x_{n-1})\}$$

in the observability co-distribution algorithm (5.9), one has,

$$\begin{aligned}
\text{span}\{dh\} &= \text{span}\{d(\delta v_1), d(\delta v_{ls_2} + v^f_{ls_2}), \cdots, d(\delta v_{ls_q} + v^f_{ls_q})\},\\
Q_0 &= \Omega_0 \cap \text{span}\{dh\} = \text{span}\{d(\delta v_1)\},\\
\bar{Q}_0 &= \sum_{i=0}^{m} L_{g_i} Q_0 + \text{span}\{dh\}\\
&= \text{span}\{d(\delta v_1), d(\delta x_1), d(\delta v_{ls_2} + v^f_{ls_2}), \cdots, d(\delta v_{ls_q} + v^f_{ls_q})\},\\
Q_1 &= \Omega_0 \cap \bar{Q}_0 = \text{span}\{d(\delta v_1), d(\delta x_1)\},\\
\bar{Q}_1 &= \sum_{i=0}^{m} L_{g_i} Q_1 + \text{span}\{dh\}\\
&= \text{span}\{d(\delta v_1), d(\delta v_2), d(\delta x_1), d(\delta v_{ls_2} + v^f_{ls_2}), \cdots, d(\delta v_{ls_q} + v^f_{ls_q})\},\\
Q_2 &= \Omega_0 \cap \bar{Q}_1 = \text{span}\{d(\delta v_1), d(\delta v_2), d(\delta x_1)\},\\
&\cdots,\\
Q_{2n-1} &= \text{span}\{d(\delta v_1), \cdots, d(\delta v_{n-1}), d(\delta x_1), \cdots, d(\delta x_{n-1})\},\\
\bar{Q}_{2n-1} &= \sum_{i=0}^{m} L_{g_i} Q_1 + \text{span}\{dh\} = \text{span}\{d(\delta v_1), \cdots, d(\delta v_n),\\
&\quad d(\delta x_1), \cdots, d(\delta x_{n-1}), d(\delta v_{ls_2} + v^f_{ls_2}), \cdots, d(\delta v_{ls_q} + v^f_{ls_q})\},\\
Q_{2n} &= \text{span}\{d(\delta v_1), \cdots, d(\delta v_n), d(\delta x_1), \cdots, d(\delta x_{n-1})\}.
\end{aligned}$$

Then $Q_k = Q_{2n}, \forall k > 2n$, which results in $o.c.a(\Omega_0) = Q_{2n} = \Omega_0$.

Considering the co-distribution $\Omega = \Omega_0 + \text{span}\{d(v^f_{ls_j})\}$, *i.e.*,

$$\Omega = \text{span}\{d(\delta v_1), \cdots, d(\delta v_n), d(\delta x_1), d(\delta x_{n-1}), d(v^f_{ls_j})\}, \forall j \in [2, q],$$

one has $o.c.a(\Omega) \supseteq o.c.a(\Omega_0)$.

Then from (5.10), one has $Q'_i \supseteq Q_i$ and $\bar{Q}'_i \supseteq \bar{Q}_i$ where $\bar{Q}'_i$ and Q'_i are the calculation results with Ω and $\bar{Q}_i$ and Q_i with Ω_0. Then one has $\bar{Q}'_{2n-1} \supseteq \bar{Q}_{2n-1}$ and furthermore

$$\begin{aligned}
Q'_{2n} &= (\Omega \cap \bar{Q}'_{2n-1})\\
&\supseteq (\Omega \cap \bar{Q}_{2n-1})\\
&= \text{span}\{d(\delta v_1), \cdots, d(\delta v_n), d(\delta x_1), d(\delta x_{n-1}), d(v^f_{ls_j})\}\\
&= \Omega,
\end{aligned}$$

which means $o.c.a(\Omega) \supseteq Q'_{2n} \supseteq \Omega$. As is known, $o.c.a(\Omega) \subseteq \Omega$, so $o.c.a(\Omega) = \Omega$.

Furthermore, one has

$$L_{g_j}\Omega \subset \Omega = \Omega + \text{span}\{dh\}, \forall j \in [0, m]. \tag{5.28}$$

The conditions in (5.11) are satisfied, *i.e.,* Ω is an observability co-distribution.

It is obvious that the vector field $p_j, j \in [2,p], j \neq i$ is in the annihilator of Ω while $\text{span}\{l\} \subset \Omega$. So it is possible to transform the train dynamics with sensor faults (5.27) into the form of (5.17), which means the possibility of fault detection of ith sensor fault.

A residual generator for the ith sensor can be in the following form,

$$\begin{aligned}
\dot{\xi}_1 &= f_{11}(\xi_1) + A_{12}\xi_2 + BU + L_{11}(y_1 - \xi_{11}) + L_{13}(y_i - \xi_{1,ls_i}),\\
\dot{\xi}_2 &= A_{21}\xi_1 + L_{21}(y_1 - \xi_{11}) + L_{23}(y_i - \xi_{1,ls_i}),\\
\dot{\xi}_3 &= -\xi_3 + L_{31}(y_1 - \xi_{11}) + L_{33}(y_i - \xi_{1,ls_i}),\\
r_i &= (y_i - \xi_{1,ls_i})/(v_r + \xi_{1,ls_i}), \qquad i \in [2,p].
\end{aligned} \tag{5.29}$$

where $\xi_1 = col(\xi_{11}, \cdots, \xi_{1n}) \in R^n, \xi_2 = col(\xi_{21}, \cdots, \xi_{2,n-1}) \in R^{n-1}, \xi_3 \in R$. In the above equation, L_{ij} are chosen by observer design approaches, such as pole placement (Luenberger observer) or optimization control (Kalman filter).

Especially, when $L_{13} = 0, L_{23} = 0$, it is also possible for the above form of dynamics to be a residual generator, because the original system without the faulty output is also observable, which has been proved in the previous chapter. It is very interesting to observe that this residual generator is naturally a fault identifier because the fault signal does not affect the states ξ_1, ξ_2, and the residual signal is actually the identifier signal of the fault. Furthermore, in this way, the residual generators and identifiers of all the sensor faults can share the same dynamics with different outputs, *i.e.,*

$$\begin{aligned}
\dot{\xi}_1 &= f_{11}(\xi_1) + A_{12}\xi_2 + BU + L_{11}(y_1 - \xi_{11}),\\
\dot{\xi}_2 &= A_{21}\xi_1 + L_{21}(y_1 - \xi_{11}),
\end{aligned} \tag{5.30}$$

and the output (a residual generator as well as a identifier) for the ith sensor fault is

$$r_i = \frac{y_2 - \xi_{1,ls_i}}{\xi_{1,ls_i} + v_r}. \tag{5.31}$$

5.4.2 Actuator fault detection and isolation

A locomotive group effort is sometimes not the same as the expected one for some reasons, such as one locomotive of the locomotive group not working. The braking efforts of wagons may be different from the expected, because of the pressure change in the braking pipe. In the following, only the fault modes as in (5.24) are studied.

When this happens, the efforts of the cars are proportional to the expected efforts, that is, the fault mode described in (5.25) is repeated as follows,

$$\begin{aligned}
\delta\dot{v} &= f_{11}(\delta v) + A_{12}\delta x + BU + B_f(U + u^o),\\
\delta\dot{x} &= A_{21}\delta v,
\end{aligned} \tag{5.32}$$

where $B_f = \text{diag}(m_f^{l_1}/m_1, \overbrace{m_f^w/m_2, \cdots, m_f^w/m_{n-1}}^{n-2}, m_f^{l_2}/m_n)$.

To detect the actuators' faults, some states are assumed to be measurable. In this study, the train is assumed to be composed of n cars with one locomotive (group) at the front and one at the rear. The wagons are between these two locomotives (locomotive groups). The speeds of the two locomotives and the two wagons next to the locomotives are also available, *i.e.*,

$$y = \begin{bmatrix} v_1 \\ v_2 \\ v_{n-1} \\ v_n \end{bmatrix}. \tag{5.33}$$

The two kinds of fault modes (sensor fault and actuator fault) are studied separately, because there are some difficulties in studying these two kinds of faults simultaneously, which will be discussed later. So, in the study of actuator faults, the speed sensors are assumed to be in good condition.

Locomotive fault detection and isolation

The locomotive group fault diagnosis is not studied in this chapter. Some approaches may be used to supervise the running states of the locomotives, such as in [69, 70, 67, 68, 71]. In this thesis, one assumes that the fault diagnosis signals and fault isolation signals are given, and when a fault happens, one's task is to reconfigure/redesign the controller.

Wagon fault detection and isolation

When the wagon faults in the system (5.32) are concerned, in the form of (5.1) for the algorithms in section 5.2, one has

$$x = \begin{bmatrix} \delta v \\ \delta x \end{bmatrix} \in R^{2n-1},$$

$$u = U,$$

$$u_f = m_f^w,$$

$$w = \begin{bmatrix} m_f^1 \\ m_f^n \end{bmatrix},$$

$$f(x) = \begin{bmatrix} f_{11}(\delta v) + A_{12}\delta x \\ A_{21}\delta v \end{bmatrix},$$

$$g(x) = B,$$

$$l = [0, (U_2 + u_2^o)/m_2, \cdots, (U_{n-1} + u_{n-1}^o)/m_{n-1}, \overbrace{0, \cdots, 0}^{n}]^T,$$
$$p_1 = [(U_1 + u_1^o)/m_1, \overbrace{0, \cdots, 0}^{n-2}, \overbrace{0, \cdots, 0}^{n}]^T,$$
$$p_2 = [\overbrace{0, \cdots, 0}^{n-1}, (U_n + u_n^o)/m_n, \overbrace{0, \cdots, 0}^{n-1}]^T,$$

and

$$h(x) = [\delta v_1, \delta v_2, \delta v_{n-1}, \delta v_n]^T.$$

According to the algorithm (5.7), one has

$$\begin{aligned} &S_0 = \bar{P} = \text{span}\{p_1, p_2\}, \\ &\bar{S}_0 \cap \ker\{dh\} = 0, \\ &\cdots, \\ &S_{k^*} = \text{span}\{p_1, p_2\}. \end{aligned}$$

from which one has

$$(\Sigma_*^P)^\perp = \text{span}\{\delta v_2, \cdots, \delta v_{n-1}, \delta x_1, \ldots, \delta x_{n-1}\}.$$

Furthermore, applying the algorithm (5.9) with $\Theta = (\Sigma_*^P)^\perp$, one has

$$\begin{aligned} \text{span}\{dh\} &= \text{span}\{d(\delta v_1), d(\delta v_2), d(\delta v_{n-1}), d(\delta v_n)\}, \\ Q_0 &= \Theta \cap \text{span}\{dh\} = \text{span}\{\delta v_2, \delta v_{n-1}\}, \\ \bar{Q}_0 &= \sum_{i=0}^{m} L_{g_i} Q_0 + \text{span}\{dh\} = \text{span}\{d(\delta v_1), d(\delta v_2), d(\delta v_{n-1}), d(\delta v_n), \\ &\quad d(k_1\delta x_1 - k_2\delta x_2), d(k_{n-2}\delta x_{n-2} - k_{n-1}\delta x_{n-1})\}, \\ Q_1 &= \Theta \cap \bar{Q}_0 = \text{span}\{d(\delta v_2), d(\delta v_{n-1}), \\ &\quad d(k_1\delta x_1 - k_2\delta x_2), d(k_{n-2}\delta x_{n-2} - k_{n-1}\delta x_{n-1})\}, \\ \bar{Q}_1 &= \sum_{i=0}^{m} L_{g_i} Q_1 + \text{span}\{dh\} \\ &= \text{span}\{d(\delta v_1), d(\delta v_2), d(\delta v_3), d(\delta v_{n-2}), d(\delta v_{n-1}), d(\delta v_n), \\ &\quad d(k_1\delta x_1 - k_2\delta x_2), d(k_{n-2}\delta x_{n-2} - k_{n-1}\delta x_{n-1})\}, \\ Q_2 &= \Theta \cap \bar{Q}_1 = \text{span}\{d(\delta v_2), d(\delta v_3), d(\delta v_{n-2}), d(\delta v_{n-1}), \\ &\quad d(k_1\delta x_1 - k_2\delta x_2), d(k_{n-2}\delta x_{n-2} - k_{n-1}\delta x_{n-1})\}, \\ &\quad \cdots, \\ Q_{k^*} &= \text{span}\{d(\delta v_2), \cdots, d(\delta v_{n-1}), d(k_1\delta x_1 - k_2\delta x_2), \\ &\quad \cdots, d(k_{n-2}\delta x_{n-2} - k_{n-1}\delta x_{n-1})\}, \end{aligned}$$

that is,

$$\begin{aligned} \Omega = o.c.a((\Sigma_*^P)^\perp) = \text{span}\{&d(\delta v_2), \cdots, d(\delta v_{n-1}), d(k_1\delta x_1 - k_2\delta x_2), \\ &\cdots, d(k_{n-2}\delta x_{n-2} - k_{n-1}\delta x_{n-1})\}. \end{aligned} \tag{5.34}$$

Repeat the above algorithm with $\Theta = \Omega$, and one has

$$\Omega = o.c.a(\Omega).$$

The second condition in (5.11) is satisfied. Then one can verify the first condition in (5.11).

$$\begin{aligned} L_g\Omega = \text{span}\{&d(k_1\delta v_1 - (k_1+k_2)\delta v_2 + k_2\delta v_3),\\ &\cdots,\\ &d(k_{n-2}\delta v_{n-2} - (k_{n-2}+k_{n-1})\delta v_{n-1} + k_{n-1}\delta v_n),\\ &d(k_1\delta x_1 - k_2\delta x_2),\\ &\cdots,\\ &d(k_{n-2}\delta x_{n-2} - k_{n-1}\delta x_{n-1})\}, \end{aligned}$$

and

$$\begin{aligned} \Omega + \text{span}\{dh\} = \text{span}\{&d(\delta v_1), d(\delta v_2), \cdots, d(\delta v_{n-2}), d(\delta v_{n-1}),\\ &d(k_1\delta x_1 - k_2\delta x_2), \cdots, d(k_{n-2}\delta x_{n-2} - k_{n-1}\delta x_{n-1})\}, \end{aligned}$$

so $L_{g_j}\Omega \subset \Omega + \text{span}\{dh\}, \forall j \in [0, m]$.

The conditions in (5.11) are satisfied with Ω defined above, which means the co-distribution Ω is the maximal observability co-distribution contained in $P^{\perp}$.

Assuming $z_{11} = \delta v_2, z_{12} = \delta v_3, \cdots, z_{1,n-2} = \delta v_{n-1}$, and $z_{1,n-1} = k_1\delta x_1 - k_2\delta x_2, \cdots, z_{1,2n-4} = k_{n-2}\delta x_{n-2} - k_{n-1}\delta x_{n-1}$, the z_1-system of (5.13) is as follows:

$$\begin{aligned} &\dot{z}_{11} = f_{11}^2(z_{11}) + z_{1,n-1}/m_2 + U_2/m_2,\\ &\cdots,\\ &\dot{z}_{1,n-2} = f_{11}^{n-1}(z_{1,n-2}) + z_{1,2n-4}/m_{n-1} + U_{n-1}/m_{n-1},\\ &z_{1,n-1} = k_1\delta v_1 - (k_1+k_2)z_{11} + k_2 z_{12},\\ &z_{1,n} = k_2 z_{11} - (k_2+k_3)z_{12} + k_3 z_{13},\\ &\cdots,\\ &z_{1,2n-5} = k_{n-3}z_{1,n-4} - (k_{n-3}+k_{n-2})z_{1,n-3} + k_{n-2}z_{1,n-2},\\ &z_{1,2n-4} = k_{n-2}z_{1,n-3} - (k_{n-2}+k_{n-1})z_{1,n-2} - k_{n-1}\delta v_n\\ &y_1 = col(z_{11}, z_{1,n-2}),\\ &y_2 = col(\delta v_1, \delta v_n). \end{aligned} \tag{5.35}$$

It can also be seen that $\text{span}\{l\} \subset \Omega$, which means the possibility of detectability of the wagon fault.

A residual generator is in the following form,

$$\begin{aligned}
\dot{\xi}_{11} &= f_{11}^2(\xi_{11}) + \xi_{21}/m_2 + U_2/m_2 + L_{11}(\xi_{11} - y_{11}) + L_{12}(\xi_{1,n-2} - y_{12}),\\
&\cdots,\\
\dot{\xi}_{1,n-2} &= f_{11}^{n-1}(\xi_{1,n-2}) + \xi_{2,n-2}/m_{n-1} + U_{n-1}/m_{n-1}\\
&\quad + L_{n-2,1}(\xi_{11} - y_{11}) + L_{n-2,2}(\xi_{1,n-2} - y_{12}),\\
\dot{\xi}_{2,1} &= k_1 y_{21} - (k_1 + k_2)\xi_{11} + k_2\xi_{12}\\
&\quad + L_{n-1,1}(\xi_{11} - y_{11}) + L_{n-1,2}(\xi_{1,n-2} - y_{12}),\\
\dot{\xi}_{2,i} &= k_i\xi_{11} - (k_i + k_{i+1})\xi_{1,i} + k_{i+1}\xi_{1,i+1}\\
&\quad + L_{i+n-2,1}(\xi_{11} - y_{11}) + L_{i+n-2,2}(\xi_{1,n-2} - y_{12}), \quad i = 2, \cdots, n-3,\\
\dot{\xi}_{2,n-2} &= k_{n-2}\xi_{1,n-3} - (k_{n-2} + k_{n-1})\xi_{1,n-2} + k_{n-1}y_{22} + L_{2n-4,1}(\xi_{11} - y_{11})\\
&\quad + L_{2n-4,2}(\xi_{1,n-2} - y_{12}),\\
y_1 &= col(\delta v_2, \delta v_{n-1}),\\
y_2 &= col(\delta v_1, \delta v_n),
\end{aligned} \tag{5.36}$$

where the matrix $L = (L_{ij})$ is suitably chosen with observer design approaches, such as pole placement (Luenberger observer) or optimization control (Kalman filter).

From (5.36), it can be seen that the dimension of the observer is $2n-4$. For a long train, n is very large. To avoid such a high-dimension observer, one considers another approach to identify the wagons' faults. The full train model is repeated as follows:

$$\begin{aligned}
m_i\dot{v}_i &= (1 - m_f^i)u_i + f_{in_{i-1}} - f_{in_i} - m_i(c_{0_i} + c_{1_i}v_i + c_{2_i}v_i^2) - f_{p_i}, \ i = 1, \cdots, n,\\
\dot{x}_j &= v_j - v_{j+1}, \qquad j = 1, \cdots, n-1,
\end{aligned} \tag{5.37}$$

where $f_{in_0} = 0, f_{in_n} = 0$.

When $m_f^i = 0$, one has reached an equilibrium (steady state, $\dot{v} = 0, \dot{x} = 0$) $v_i = v_r, i = 1, \cdots, n$, and $f_{in_j}^0(x_j^0)$, with $u_i = u_i^0$.

$$\begin{aligned}
\dot{v}_r &= u_i^0 + f_{in_{i-1}}^0 - f_{in_i}^0 - m_i(c_{0_i} + c_{1_i}v_r + c_{2_i}v_r^2) - f_{p_i}, \qquad i = 1, \cdots, n,\\
\dot{x}_j^0 &= v_r - v_r, j = 1, \cdots, n-1.
\end{aligned} \tag{5.38}$$

Thus one has a difference system (5.21) with $\delta v_i = v_i - v_r, \delta x_j = x_j - x_j^0$, which is also denoted as follows,

$$\dot{X} = f(X) + BU. \tag{5.39}$$

A speed regulator designed in the previous chapter for this difference system is repeated as follows,

$$\begin{aligned}
\dot{z} &= f(z) + BU + G_1(y_m - C_m z),\\
U &= c(w) + K(z - \pi(w)),
\end{aligned} \tag{5.40}$$

The closed-loop dynamics are

$$\begin{aligned} \dot{X} &= f(X) + BU, \\ \dot{z} &= f(z) + BU + G_1(y_m - C_m z), \\ U &= c(w) + K(z - \pi(w)). \end{aligned} \tag{5.41}$$

When the train is faultless, the train speed will track the reference speed under the above controller. How are the train's dynamics when $m_f^i \neq 0$? One first checks whether the train dynamics are stable. If they are, then one will study the new steady states.

The locomotives' faults are assumed to be detected and isolated through other approaches, so only the faults of the wagons with $m_f^i = m_f^w, i = 2, \cdots, n-1$ are considered in the following identification.

When $m_f^w \neq 0$, the closed-loop dynamics (5.41) in cruise phase is as follows

$$\begin{aligned} \dot{X} &= f(X) + BU - B_f(U + u^o), \\ \dot{z} &= f(z) + BU + G_1(y_m - C_m z), \\ U &= Kz, \end{aligned} \tag{5.42}$$

where $B_f = \text{diag}(0, \overbrace{m_f^w/m_2, \cdots, m_f^w/m_{n-1}}^{n-2}, \overbrace{0, \cdots, 0}^{n})$.

Assuming $A = \frac{\partial f(0)}{\partial X}$, (from the above, one knows $A + BK < 0, A + G_1 C_m < 0$,) one has a linearized model as follows:

$$\begin{aligned} \dot{X} &= AX + (B - B_f)Kz - B_f u^o, \\ \dot{z} &= -GC_m X + (A + G_1 C_m + BK)z. \end{aligned} \tag{5.43}$$

If the K, G are chosen such that

$$\begin{bmatrix} A & (B - B_f)K \\ -GC & A + GC + BK \end{bmatrix} < 0,$$

then the above system (5.43) is stable.

The steady state of the train can be denoted as $(\dot{v} = 0, \dot{x} = 0)$ $v_i = v_r^f, i = 1, \cdots, n$, and $f_{in_j}^f(x_j^f)$, with u_i,

$$\begin{aligned} m_1 \dot{v}_r^f &= u_1 - f_{in_1}^f - m_1(c_{0_1} + c_{1_1} v_r^f + c_{2_1}(v_r^f)^2) - f_{p_1}, \\ m_i \dot{v}_r^f &= u_i + f_{in_{i-1}}^f - f_{in_i}^f - m_i(c_{0_i} + c_{1_i} v_r^f + c_{2_i}(v_r^f)^2) - f_{p_i} - m_f^i u_i, i = 2, \cdots, n-1, \\ m_n \dot{v}_r^f &= u_n + f_{in_n}^f - m_n(c_{0_n} + c_{1_n} v_r^f + c_{2_n}(v_r^f)^2) - f_{p_n}, \end{aligned} \tag{5.44}$$

The locomotive fault is identifiable with other approaches and only the fault of wagons with $m_f^i = m_f^w, 2, \cdots, n-1$ is considered. Furthermore if v_r^f is known, then there are only n unknown variables $f_{in_i}^f, i = 1, \cdots, n-1, m_f^w$ in the above n equations. Especially when summing up the first n equations, one has

$$0 = \sum_{i=1}^{n} u_i - \sum_{i=1}^{n} m_i(c_{0_i} + c_{1_i} v_r^f + c_{2_i}(v_r^f)^2) - \sum_{i=1}^{n} f_{p_i} - \sum_{j=2}^{n-1} m_f^i u_i. \tag{5.45}$$

It is possible to solve them, which means the identifiability of the wagon fault.

Although it is impossible for a train to reach steady states in practical running, it is practical to assume that the train can approximate its steady state, at least within a cruise phase. The practical steady-state speed of the running train is defined with the analysis of differences of the measurable speeds (v_1, v_2, v_{n-1}, v_n) in this chapter.

When all the wagon are faultless and the train is running in its steady state, one has,

$$0 = \sum_{i=1}^{n} u_i^o - \sum_{i=1}^{n} \left(m_i(c_{0_i} + c_{1_i} v_r + c_{2_i}(v_r)^2) + f_{p_i} \right). \tag{5.46}$$

With (5.45) and (5.46), if all the wagons' faults are the same, *i.e.*, $m_f^i = m_f^w, i = 2, \cdots, n-1$, one has

$$(1 - m_f^w) \sum_{i=1}^{n} u_i - \sum_{i=1}^{n} u_i^o = \sum_{i=1}^{n} m_i \left(c_{1_i} v_r^f + c_{2_i}(v_r^f)^2 - (c_{1_i} v_r + c_{2_i} v_r^2) \right), \tag{5.47}$$

from which one can get m_f^w.

5.5 Fault-tolerant control (FTC)

5.5.1 FDI and FTC in the case of sensor faults

The residual generator in the case of sensor faults is as in equations (5.30) and (5.31), where function f_{11} is linearized and thus the observer is a linear system. The matrices L_{11}, L_{21} are determined through the function LQR in MATLAB. If the sensor fault model is linearized as

$$\begin{aligned} \dot{z} &= Az + BU, \\ y_m &= C_m z, \\ y_i &= (1 + m_{v_i}^f) v_i - v_r, \qquad i = 2, \cdots, p, \end{aligned} \tag{5.48}$$

then one assumes $C_{m1} = C_m(1,:)$, $Q = I_{(2n-1)\times(2n-1)}$, $R = 1$, and with the function $L = lqr(A', C_{m1}', Q, R)$, $L = L'$, one gets the residual generator.

In the controller, one assumes the outputs of the residual generator are $\bar{v}_i$ and the measured speeds v_{mi}. The reference speed is v_r. In the control process, for the output v_{mi} of the ith speed sensor, one will take $K_i^{sensor} \times v_{mi}$ as the real speed of the corresponding car, where K_i^{sensor} is a coefficient, which will be modified when the sensor fault is detected and isolated. A constant V_{th} is set as the threshold of fault diagnosis. For the fault detection and isolation, one has other arrays in the programme, $KD_{i,1:11}^{sensor}, Nsensor_i$. The former is used to store the past 11 coefficients of the sensor and the latter the times of continuous violations of the fault-free condition.

The fault detection and isolation programme is shown as Fig. 5.1, where $KD_{i,1:11}^{sensor} = 0_{1\times 11}, N_i^{sensor} = 0$ and $K_i^{sensor} = 1$ are initialized. This programme is executed once a second.

It is known that there is a possibility of false rejections and a possibility of false acceptances for a fault-tolerant controller, which should be considered. The first possibility is that it does not detect or isolate the fault well when a fault occurs. The second is that it takes a faultless system as a fault system. The choice of the thresholds affect these two possibilities. Generally, when one possibility is reduced with a set of thresholds, the other one is increased. When the threshold is to be determined, the balance between the two possibilities should be considered. From Fig. 5.1, it is impossible to avoid the above two possibilities. However, the effects of the possibility of false acceptance can be discussed qualitatively. If a fault is falsely accepted, for example, a sensor with a gain 1 is falsely identified with a gain 1.05, then with the FTC, the speed of the train will be underestimated, and thus the train will be overspeed. In that case, the FDI will further identify a gain fault lower than 1 to correct the false acceptance. It is in the way of "negative feedback" to track the real value of the gain. Such an approach in Fig. 5.1 does not obviously affect the train performance. That can be seen from the simulation results of an FTC in a faultless system.

In this thesis, the two possibilities from theoretic viewpoints will not be discussed, nor will the time delay between the fault occurrence and fault isolation. Instead, they will be discussed on the basis of the simulation results.

5.5.2 Controller redesign in the case of a locomotive fault

As described before, fault detection and isolation of locomotive faults are not studied in this thesis. Here, only the fault-tolerant control of a locomotive fault is considered.

In the following simulation, one assumes the fault is detected and identified 60 seconds after it occurs. When it is identified, the controller will be redesigned. According to the fault, the parameters of the train are modified and then the controller is redesigned with the new parameters. For example, assuming the coefficient of its input in the train model is $Bt(i,:)$, if the locomotive group $u(i)$ loses half its effort, the new coefficient is $Bt(i,:)/2$.

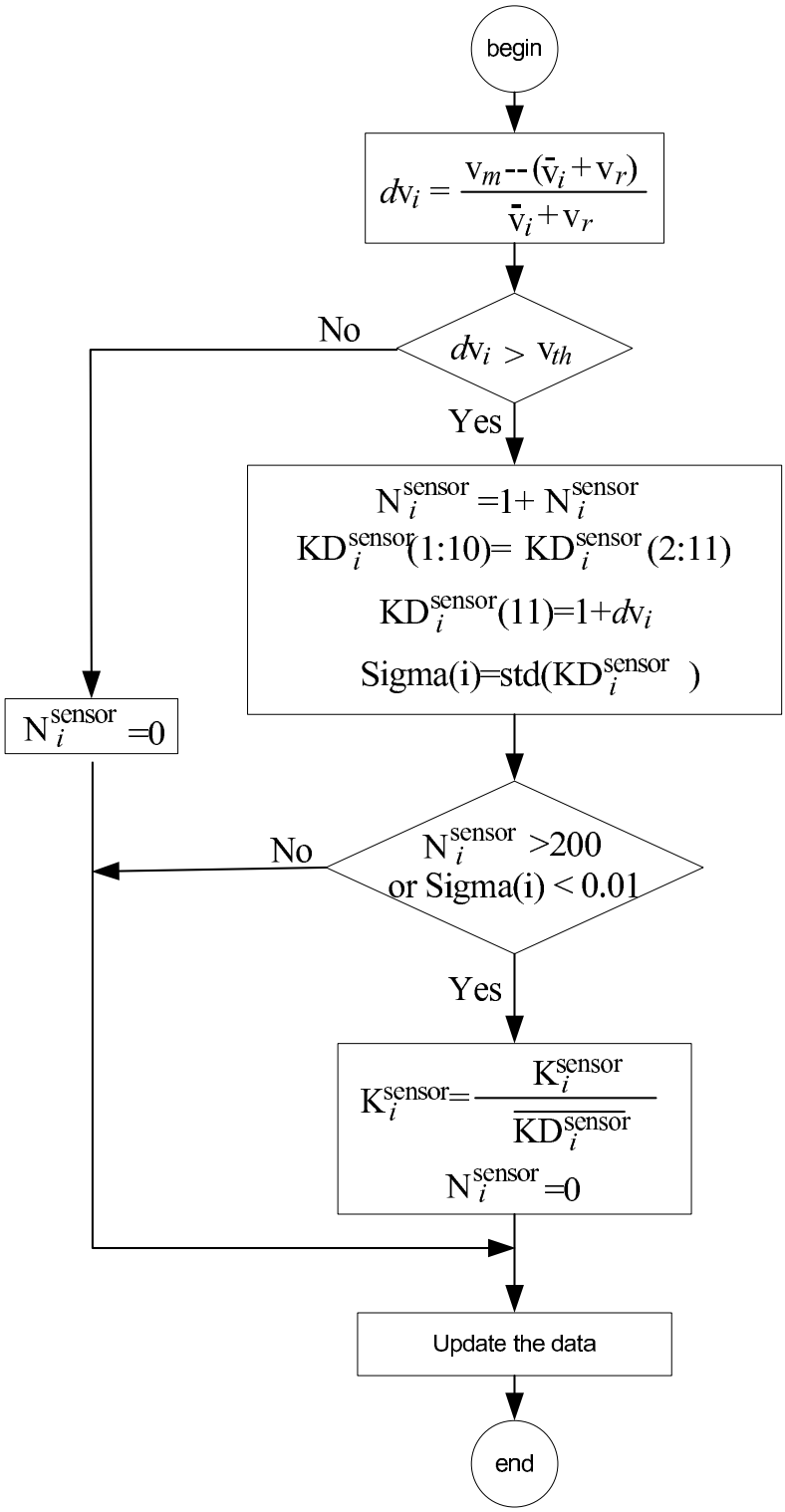

Figure 5.1: Sensor fault detection and isolation programme

5.5.3 FDI and FTC in the case of a wagon fault

When a wagon fault is detected and identified, similar to the case of a locomotive fault, the controller will be redesigned according to the updated parameters of the train. The key is fault detection and isolation. In the current simulation, this is done following the approach proposed in section 5.4.2.

In this approach, one employs the algorithm as Fig. 5.2 to detect and identify the fault; this is executed once a second. In the figure, the matrix Bb is the coefficient matrix of the brake inputs in the train model, which is equal to $\text{diag}(1/m_i)$ when the braking system is faultless. The variables v_m, v_r are the measured speed and reference speed, respectively. The variable K^f_{brake} is a ten-dimension array used to store the past ten estimated fault signals, while N^f_{brake} is a counter number of the continuous violation of fault condition.

There are the same possibilities in the FDI of a wagon fault as in the FDI of a sensor fault. Similar to the latter, the FDI of wagon faults is also "negative feedback" to track the real value of the wagon actuator. The effect of false acceptance on the train performance will not be discussed in a theoretic way, but is discussed with the simulation results. The time delay between the fault occurrence and fault isolation will not be discussed either.

5.6 Simulation

The simulation setting of the train is the same as previous chapters as well as the speed profile and track profile. When all sensors and actuators are faultless, the controller is the speed regulator with $K_e = 1, K_f = 1, K_v = 1$, designed in part 4.3. When a fault occurs, the controller will be redesigned. The controller redesign includes two parts: the redesign of the optimal scheduling and the redesign of the speed regulator.

5.6.1 Simulation of sensor faults

In simulation, the sensor fault detection and isolation programme is only working during the cruise phase. The simulation setting is the same as in section 4.3. The fault diagnosis parameter setting is as in Fig. 5.1.

There are two kinds of errors with the gains of speed sensors. One is a random error, which depends on the accuracy of speed sensor. The other one is a systematic error with gain, which is a real fault and should be corrected. From the simulation, it will be seen that the former has little impact on the performance of controllers, while

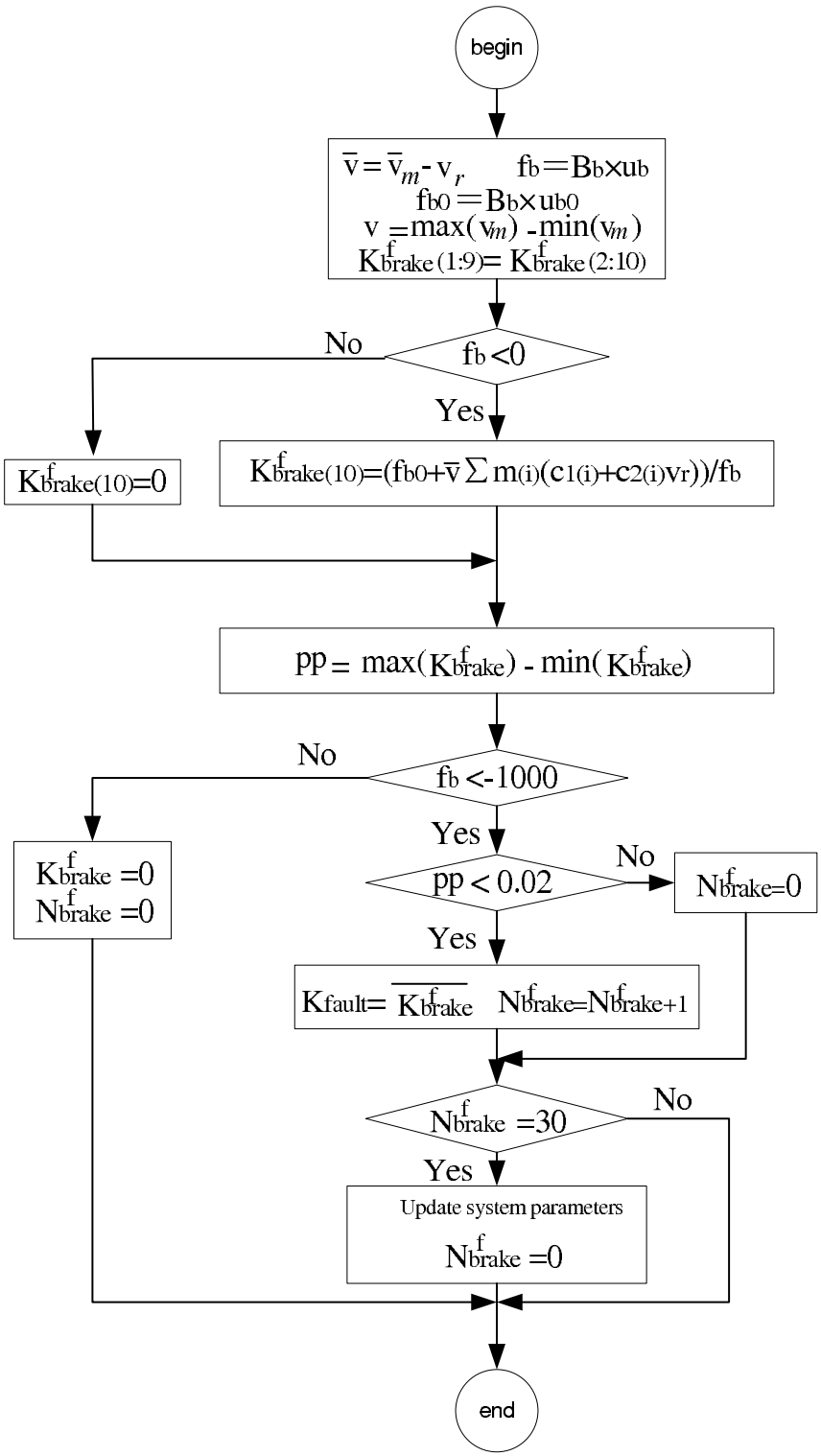

Figure 5.2: Wagon fault detection and isolation programme

the latter has much greater impact.

In the following description, the accuracy $1\pm\alpha\%$ of a speed sensor means the output of the sensor is randomly $1 \pm \alpha\%$ of the measured speed, while the gain fault $\beta\%$ of a sensor means the output of the sensor is $1 + \beta\%$ of the measured speed with the accuracy 1.

The effects of the random errors of the speed sensors on the non-FTC (a controller without fault-tolerant capacity) and the FTC (a controller with fault-tolerant capacity) are discussed firstly. The following three groups of figures are the simulation results with non-FTC of a faultless system, FTC of a faultless system and FTC of a faulty system, respectively.

Fig. 5.3 and Fig. 5.4 are the simulation results of a faultless system with non-FTC. All sensors in the former case have accuracies of 100%, while those in the latter have accuracies of $1 \pm 5\%$ from the beginning.

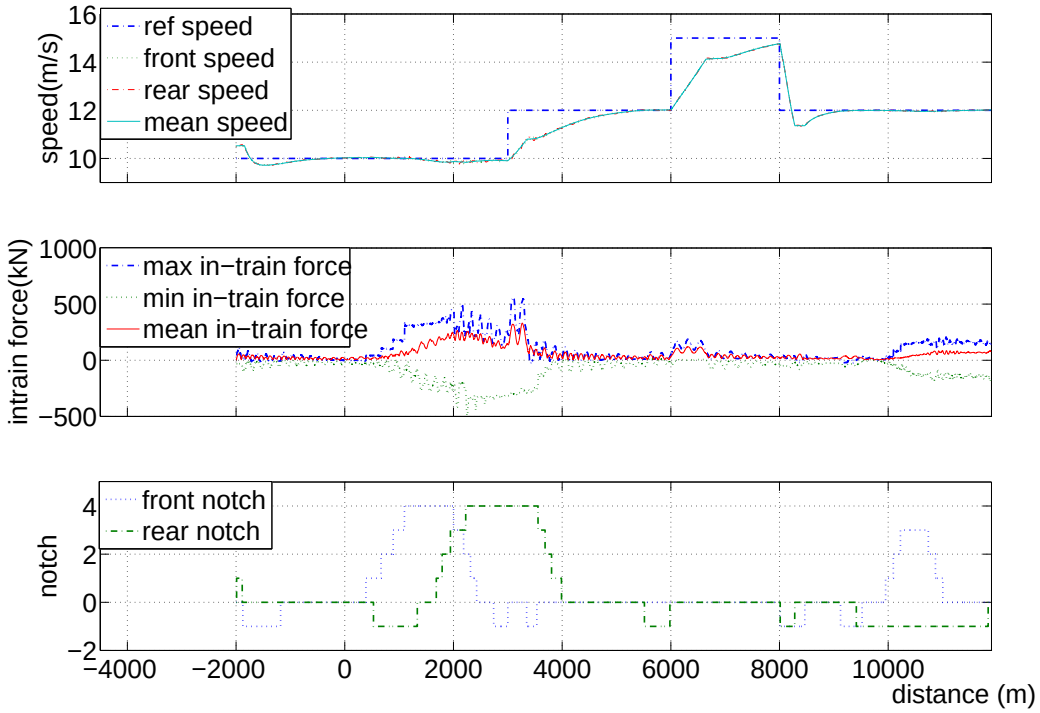

Figure 5.3: Non-FTC (sensor accuracy of 100%)

Fig. 5.5 and Fig. 5.6 are simulation results of a faultless system with an FTC. All sensors in the former case have accuracies of 100%, while those in the latter have accuracies of $1 \pm 5\%$ from the beginning.

Fig. 5.7 and Fig. 5.8 are the simulation results of a faulty system (the second sensor

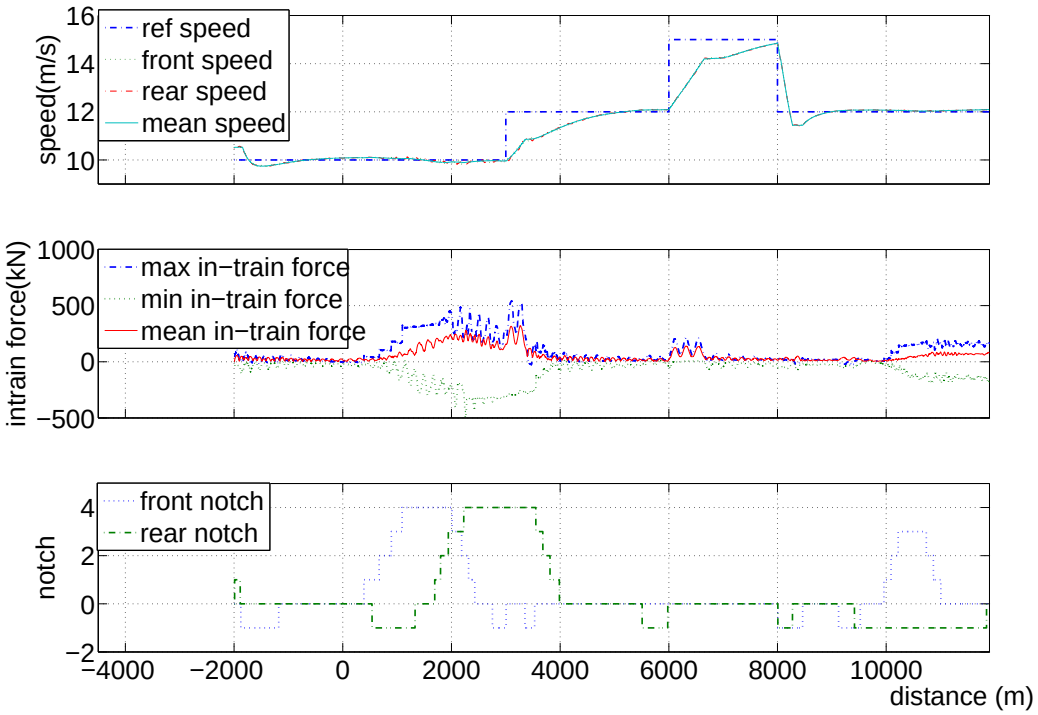

Figure 5.4: Non-FTC (sensor accuracy of $1 \pm 5\%$)

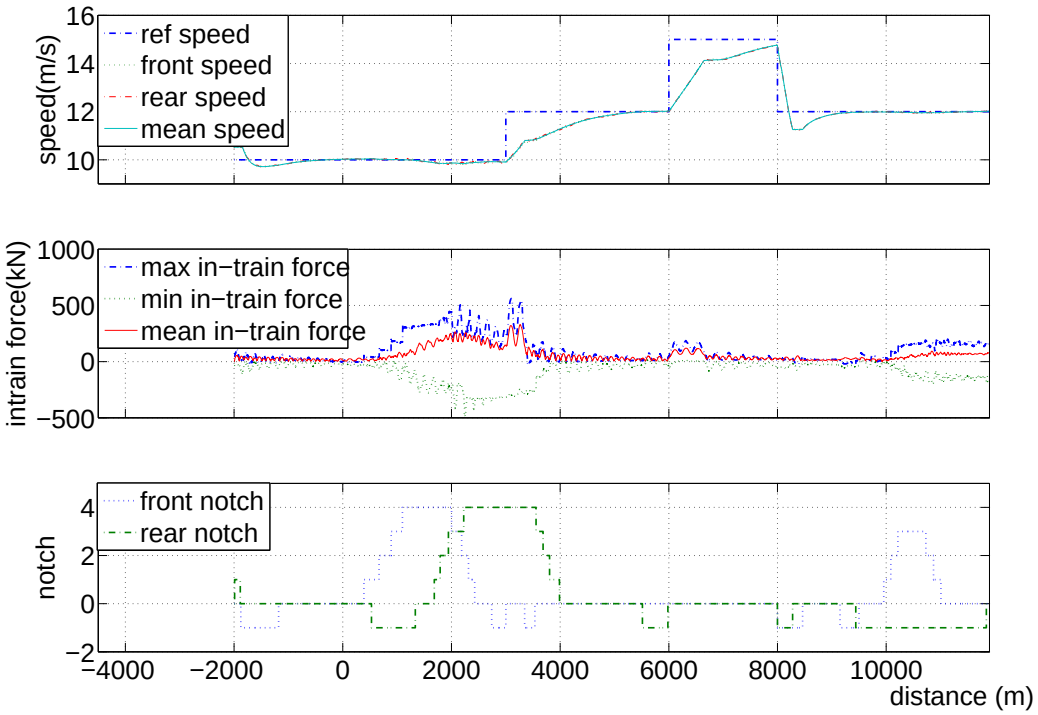

Figure 5.5: FTC (sensor accuracy of 100%)

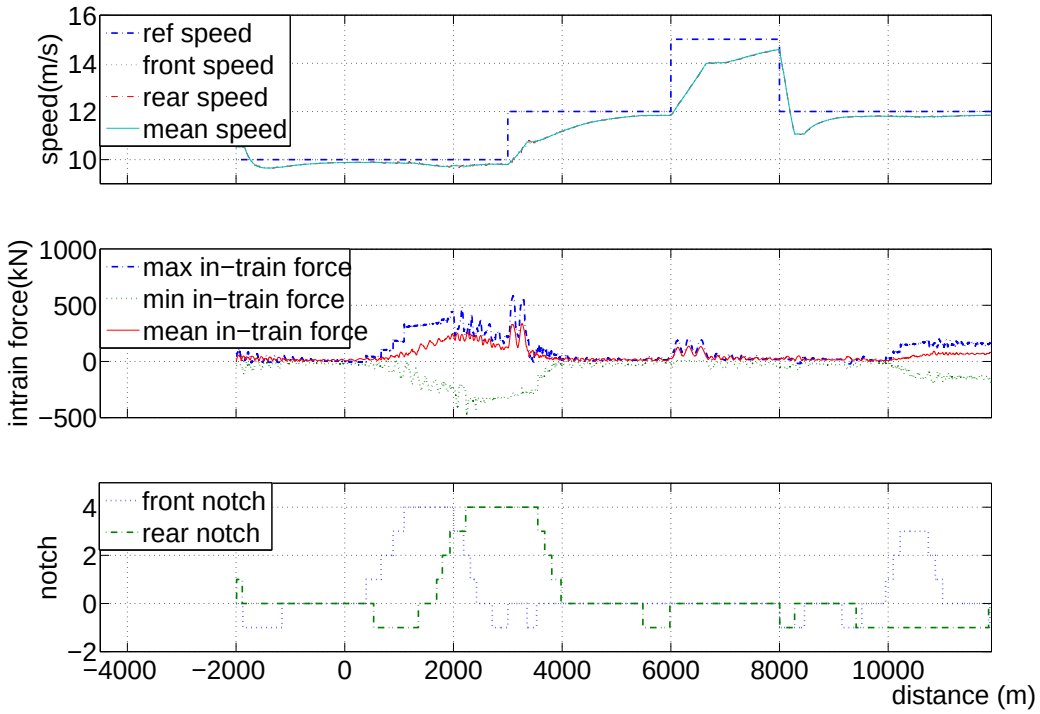

Figure 5.6: FTC (sensor accuracy of $1 \pm 5\%$)

is faulty with a gain fault +5%). All sensors in the former case have accuracies of 100% while those in the latter have accuracies of $1 \pm 5\%$.

Comparing Fig. 5.3 with Fig. 5.4, one can see that the random error has very little effect on the speed regulators without fault-tolerant capacity when there is no fault with the sensors. Comparing Fig. 5.5 with Fig. 5.6, it can be seen that the random error makes the performance a little worse with the fault-tolerant controller even though no fault occurs. The effects are, however, very small. The performance index is referred to in Table 5.1. From a comparison of Fig. 5.7 with Fig. 5.8, one sees that the random errors of sensors have little impact on the performance of the fault-tolerant controllers when a fault occurs with the second sensor. From a comparison of the last two pairs, it is concluded that random errors have effects on the performance of the fault-tolerant controllers, but the effects are limited. The result is still acceptable. In the following simulation of this study, one therefore seldom considers the random errors of the sensors. From the above discussion, it is clear the results are not affected.

A discussion of the effects of the FTC on the performance of a speed regulator is as below.

The figures from Fig. 5.3 to Fig. 5.9 are compared. Fig. 5.9 is the simulation result of a faulty system (the second sensor is faulty with a gain fault +5%) with all sensors having accuracies of $1 \pm 5\%$. The controller in this simulation is a non-FTC.

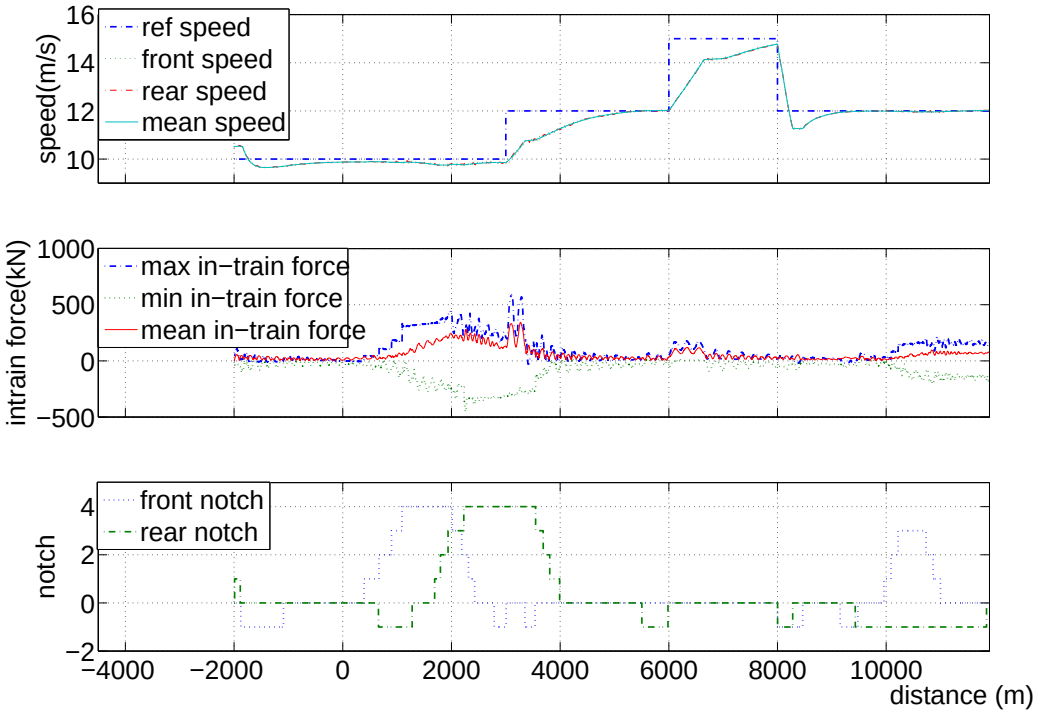

Figure 5.7: FTC (sensor accuracy of $1 + 0\%$ and second sensor gain fault of $+5\%$)

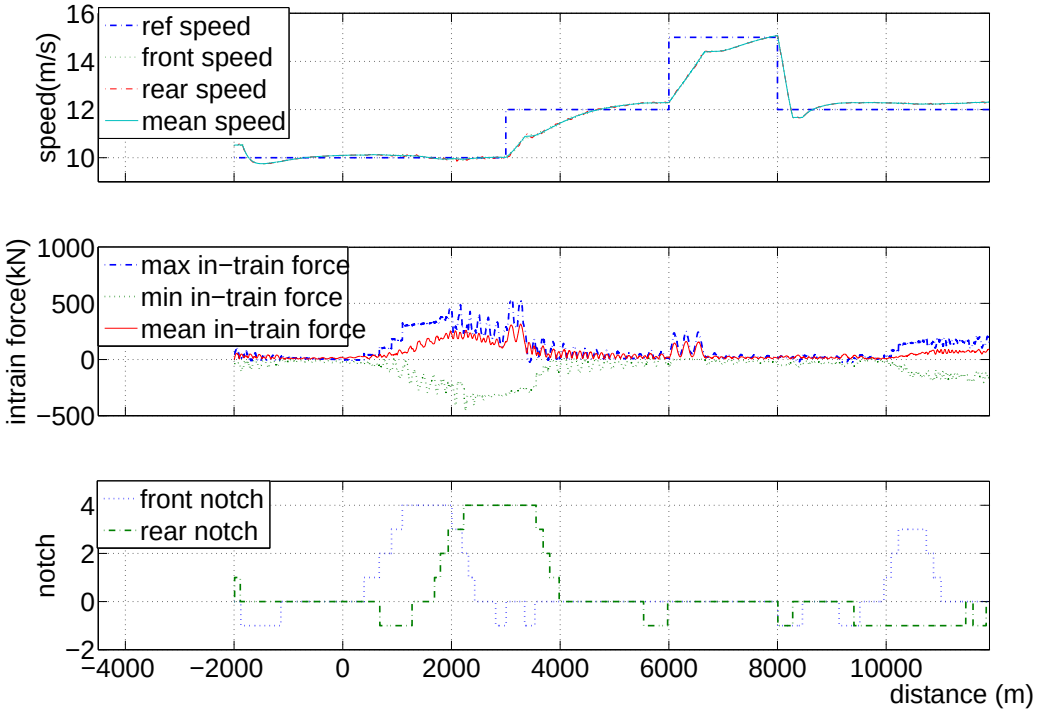

Figure 5.8: FTC (sensor accuracy of $1 \pm 5\%$ and second sensor gain fault of $+5\%$)

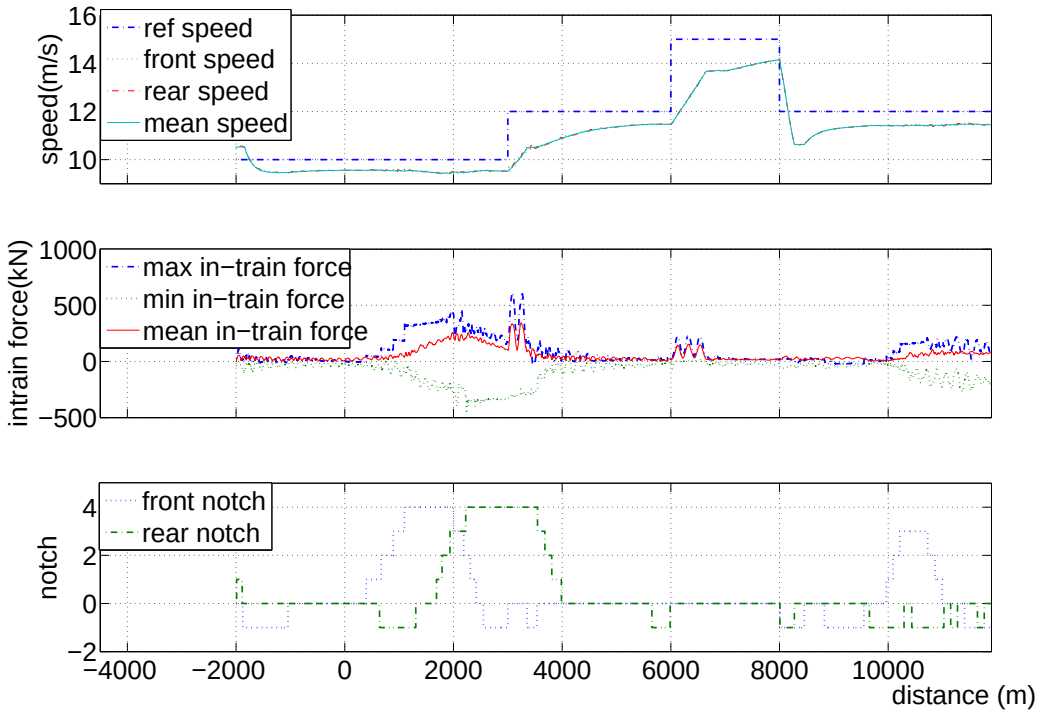

Figure 5.9: Non-FTC (sensor accuracy of $1 \pm 5\%$ and 2^{nd} sensor gain fault of $+5\%$)

One first compares Fig. 5.3 with Fig. 5.5, in which the sensors have accuracies of 100% and the system is faultless. The former is controlled with a non-FTC while the latter is controlled with an FTC. From these two figures, one can see that the performance is visually very similar although from Table 5.1 the last one appears to be slightly worse.

Then Fig. 5.4 is compared with Fig. 5.6, in which the sensors have accuracies of $1 \pm 5\%$ and the system is faultless. The former is controlled with a non-FTC while the latter is controlled with an FTC. The speed performance of the latter is a little worse than that of the former, and even the latter has a steady speed error. This is because the random errors of the sensors have an effect on the performance of an FTC. Even so, the FTC does not explicitly worsen the performance of the speed regulator. The result is still acceptable.

The advantage of an FTC can be seen when a fault occurs. Fig. 5.9 and Fig. 5.8 represent simulation of a faulty system (all sensors with accuracies of $1 \pm 5\%$ and the second one has a gain fault of $+5\%$) with a non-FTC and with an FTC, respectively. It is seen that the speed performance of the latter is obviously better than that of the former. That is the contribution of the FTC. From the above comparison, one can conclude that

1) When no fault occurs and all sensors have accuracies of 100%, the speed perfor-

mance of an FTC is very similar to that of a non-FTC.

2) When no fault occurs and all sensors have accuracies of $1 \pm 5\%$, the speed performance of an FTC is a little worse than that of a non-FTC. However, the result is still thought as a good result.

3) When a small fault (the second sensor has a gain fault of $+5\%$) occurs and all sensors have accuracies of $1 \pm 5\%$, the speed performance of an FTC is much better than that of a non-FTC.

From the above, it is concluded that the FTC for the sensors' faults is suitable.

In the above simulations, only the FTC for the second sensor fault is given. In the following, one can see the FTC applied in the faults of the third and fourth sensors, and in the concurrent faults of the second and fourth ones. Since the accuracy of a sensor does not explicitly affect the performance of the controller, without a special description, the sensor accuracy is assumed to be 100% in the rest of this thesis.

Fig. 5.10 shows an FTC with the third sensor having a gain fault of $+7\%$ from the beginning. Fig. 5.11 shows an FTC with the fourth sensor having a gain fault of -20% from the beginning. Fig. 5.12 shows an FTC with the fourth sensor having a gain fault of $+20\%$ from the beginning.

A kind of concurrent fault (the second sensor has a gain fault of $+43\%$ and the fourth one has a gain fault of $+12\%$ from the beginning) is shown in Fig. 5.13 with an FTC. Another kind of concurrent fault (the second sensor has a gain fault of $+30\%$ from the distance of $2,000$ m and the fourth one has a gain fault of -30% from the distance of $4,000$ m) is shown in Fig. 5.14 with an FTC.

The comparison of these figures in performance is shown in Table 5.1. The statistical items are the same as those in the Table 4.1.

From an analysis of the figures and a comparison with Table 5.1, one can conclude that the application of FTC of sensor faults in the speed regulation explicitly improves performance in the case of fault occurrence and does not explicitly worsen performance in the case of a faultless train.

5.6.2 Simulation of locomotive faults

In the previous parts, fault detection and isolation of locomotive faults are assumed to be done by other approaches and only fault-tolerant control is considered in this thesis. The fault signal is assumed to be given when a fault occurs.

In the train setting of simulation, there are two groups of locomotives at the front

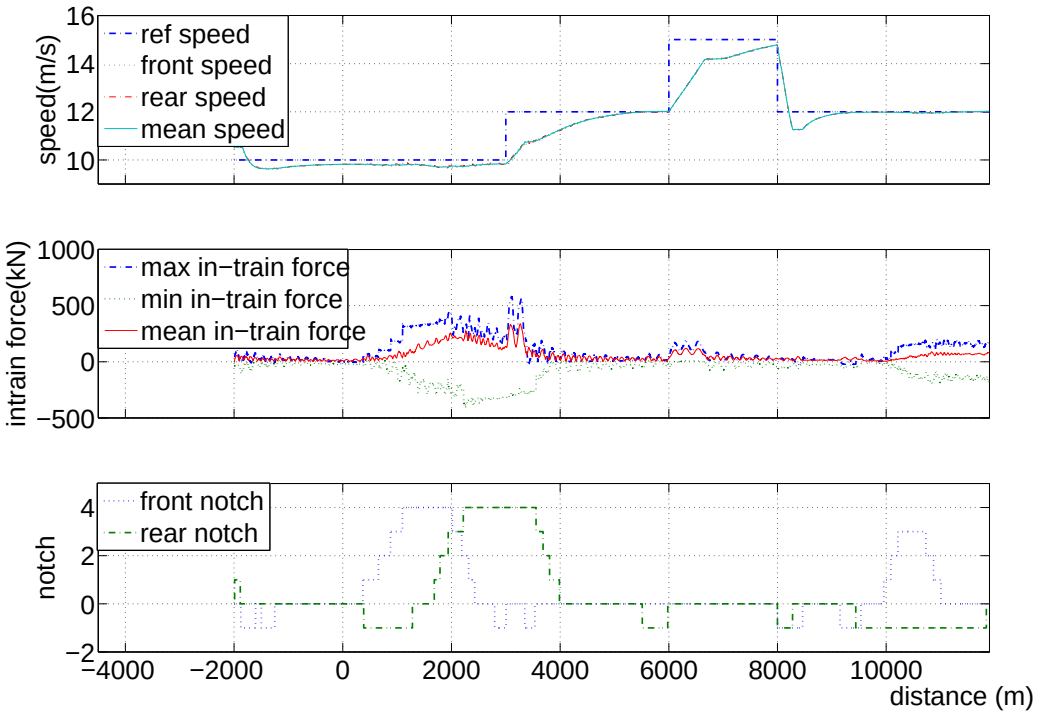

Figure 5.10: FTC (third sensor with a gain fault of +7%)

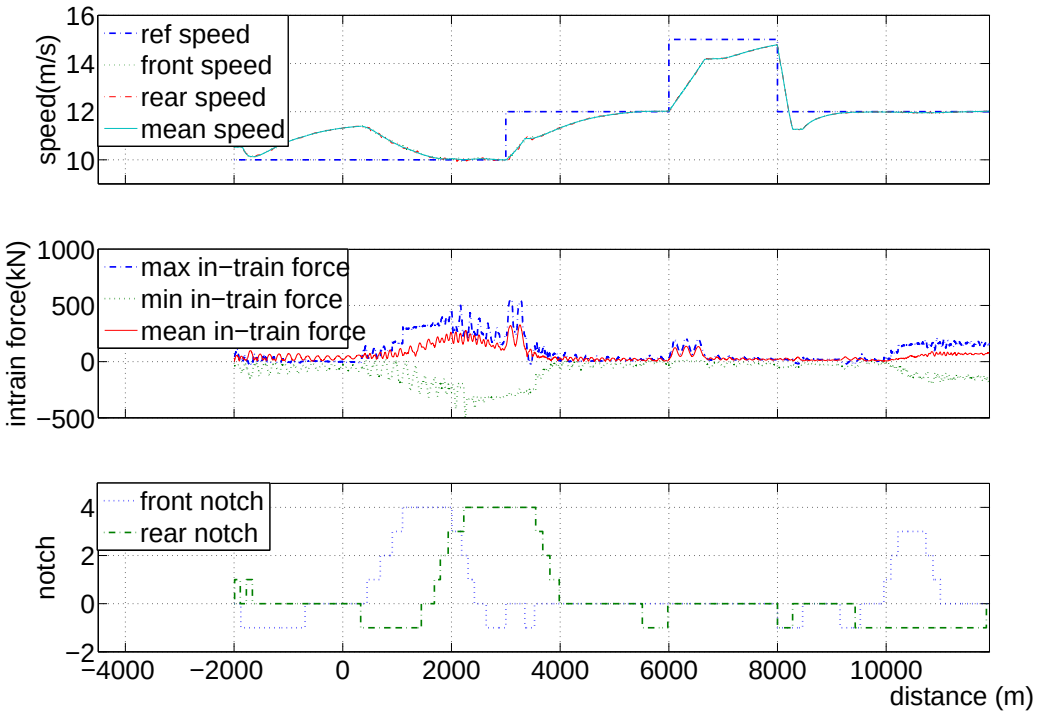

Figure 5.11: FTC (fourth sensor with a gain fault of −20%)

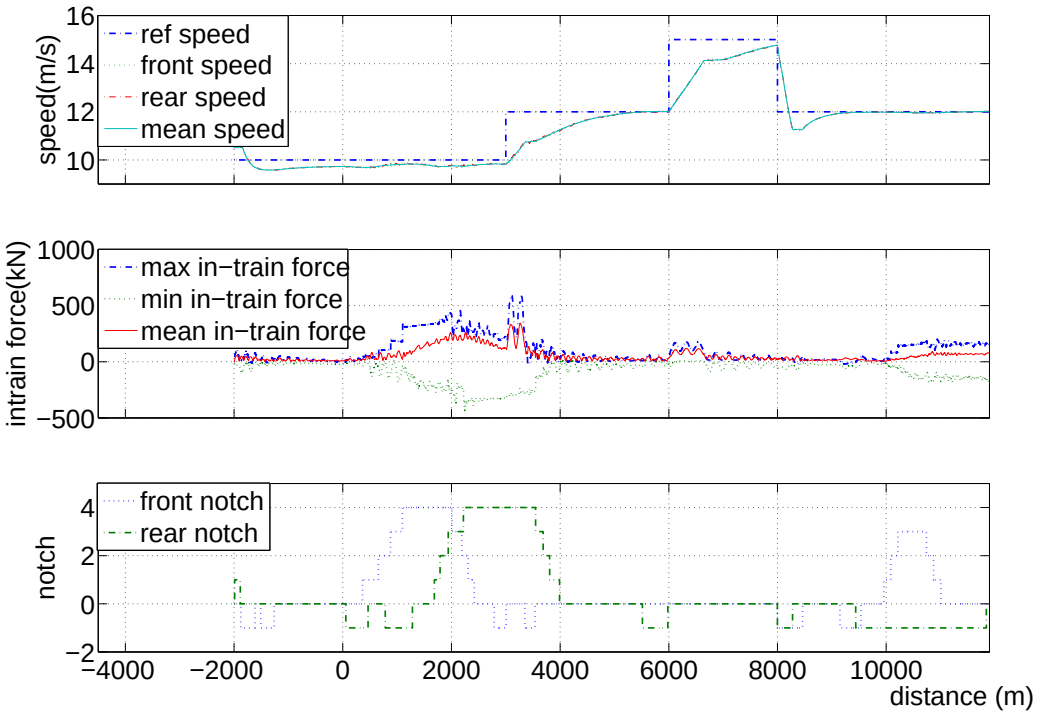

Figure 5.12: FTC (fourth sensor with a gain fault of +20%)

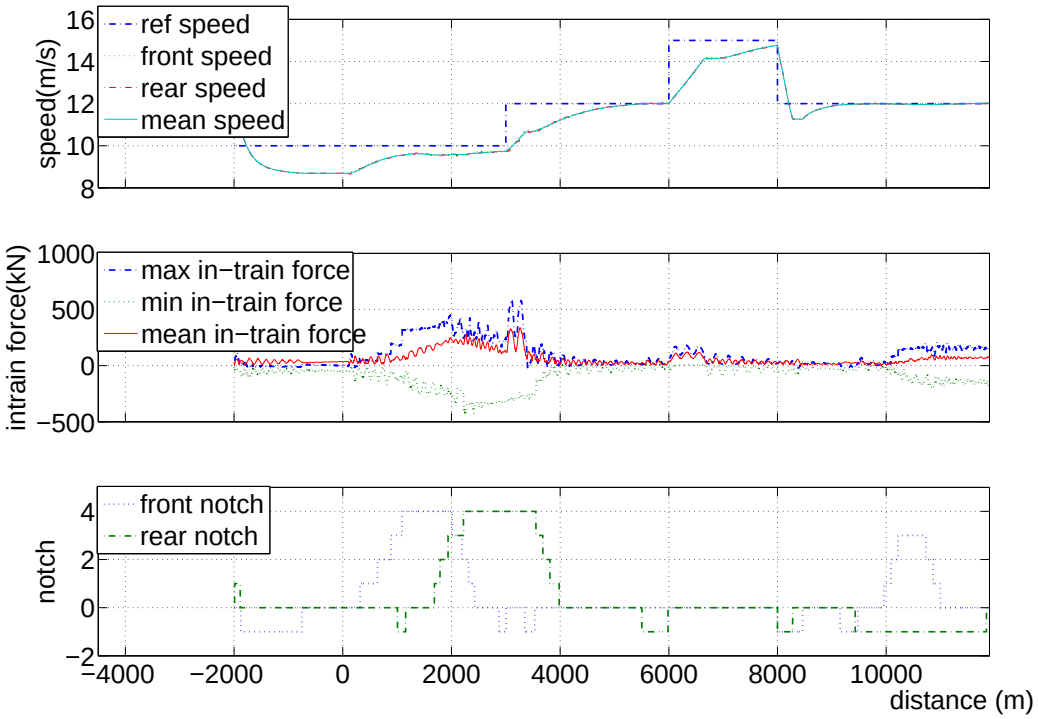

Figure 5.13: FTC (concurrent faults)

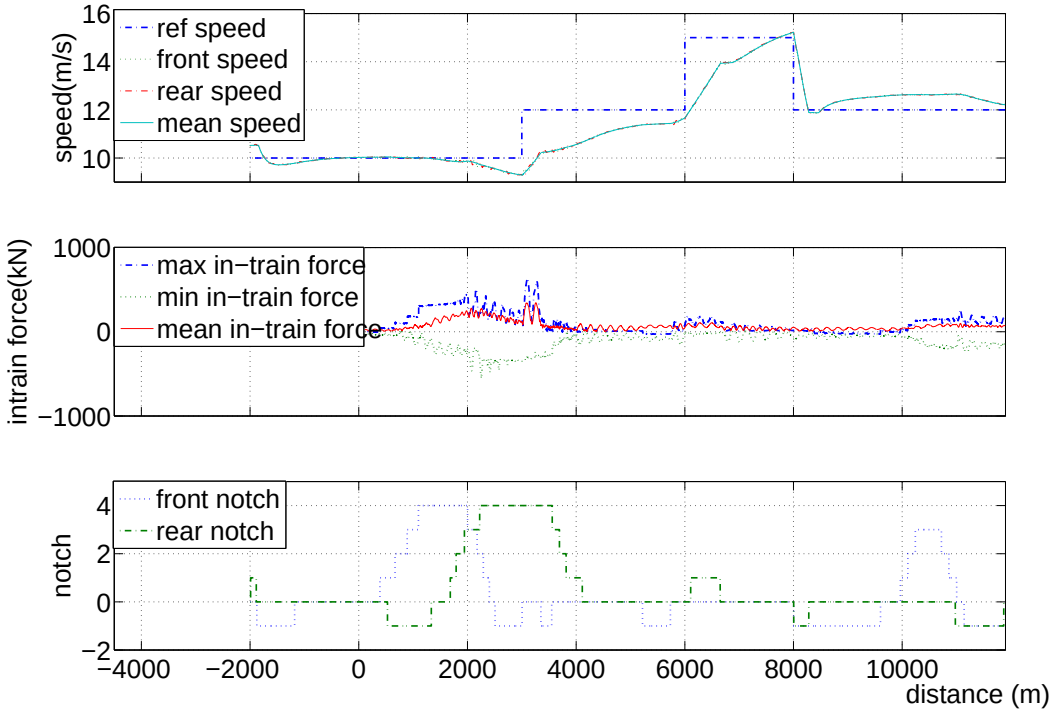

Figure 5.14: FTC (concurrent faults)

Table 5.1: Comparison of non-FTC and FTC of sensor faults

	$\lvert\delta\bar{v}\rvert$(m/s)			$\overline{\lvert f_{in}\rvert}$(kN)			E
	max	mean	std	max	mean	std	(MJ)
Fig. 5.3	2.9813	0.3277	0.5321	331.1579	58.5970	63.0519	12,400
Fig. 5.4	2.9102	0.3163	0.5129	323.3944	56.4624	63.8505	12,200
Fig. 5.9	3.5348	0.7831	0.5225	343.8927	57.7336	63.6908	13,100
Fig. 5.8	3.0783	0.3329	0.4672	316.3416	59.3843	65.0268	12,600
Fig. 5.7	2.9780	0.3718	0.5181	343.3660	59.7467	63.4535	12,900
Fig. 5.5	2.9812	0.3324	0.5288	331.1538	59.5132	63.5522	12,800
Fig. 5.6	3.1587	0.4667	0.5230	338.3691	55.7556	65.5126	13,200
Fig. 5.10	2.9825	0.3902	0.5132	338.7165	58.7065	64.1423	13,000
Fig. 5.11	2.9782	0.5067	0.5788	28.4991	60.5036	63.3990	12,600
Fig. 5.12	2.9810	0.4066	0.5102	343.1219	58.9628	64.1343	13,100
Fig. 5.13	2.9840	0.6170	0.5842	336.3811	63.6549	62.9222	13,400
Fig. 5.14	3.3412	0.6047	0.6593	345.4785	65.6464	62.0612	13,500

and at the rear, respectively. Every group is composed of two locomotives. In simulation of an FTC, one assumes that the fault is that one locomotive in a locomotive group does not work. When the two locomotive in a group do not work, distributed power control cannot apply, which is not discussed in this study. So, in the simulation, it is assumed that the fault is detected 60 second after it happens and the controller is then redesigned. There are three types of faults:

1) Front-loco-fault: one locomotive of the front locomotive group does not work;

2) Rear-loco-fault: one locomotive of the rear locomotive group does not work;

3) Both-loco-fault: one locomotive of the front locomotive group and one of the rear group do not work;

Fig. 5.15 and Fig. 5.16 are simulation results of Front-loco-fault with an FTC and a non-FTC, respectively. One of the locomotives at the front does not work from the distance $1,500m$.

Fig. 5.17 and Fig. 5.18 are simulation results of rear-loco-fault with an FTC and a non-FTC, respectively. One of the locomotives at the rear does not work from the distance $1,500m$.

Fig. 5.19 and Fig. 5.20 are simulation results of Both-loco-fault with an FTC and a non-FTC, respectively. One locomotive at the front and one at the rear do not work from the distance $1,500m$.

From comparing Fig. 5.15 and Fig. 5.16, it can be seen that the performance of an FTC is better than that of a non-FTC during the period when the train is passing over a hill. (In these figures, the track profile is the same as that of previous simulation and is not shown.) That can also be seen from the front locomotive effort. When the effort of the front locomotive group is zero, then there is no difference between the FTC and non-FTC. When the front locomotive group uses traction power, the speed performance of the FTC is better.

The above conclusion is also clear from a comparison of Fig. 5.17 with Fig. 5.18 and Fig. 5.19 with Fig. 5.20. The performance comparison of these figures is shown in Table 5.2.

The advantage of an FTC in the locomotive fault does not seem obvious in the above simulation. This is because the locomotive groups make no effort (unpowered) during most of the travel period. When the locomotive groups make efforts, the advantage is obvious.

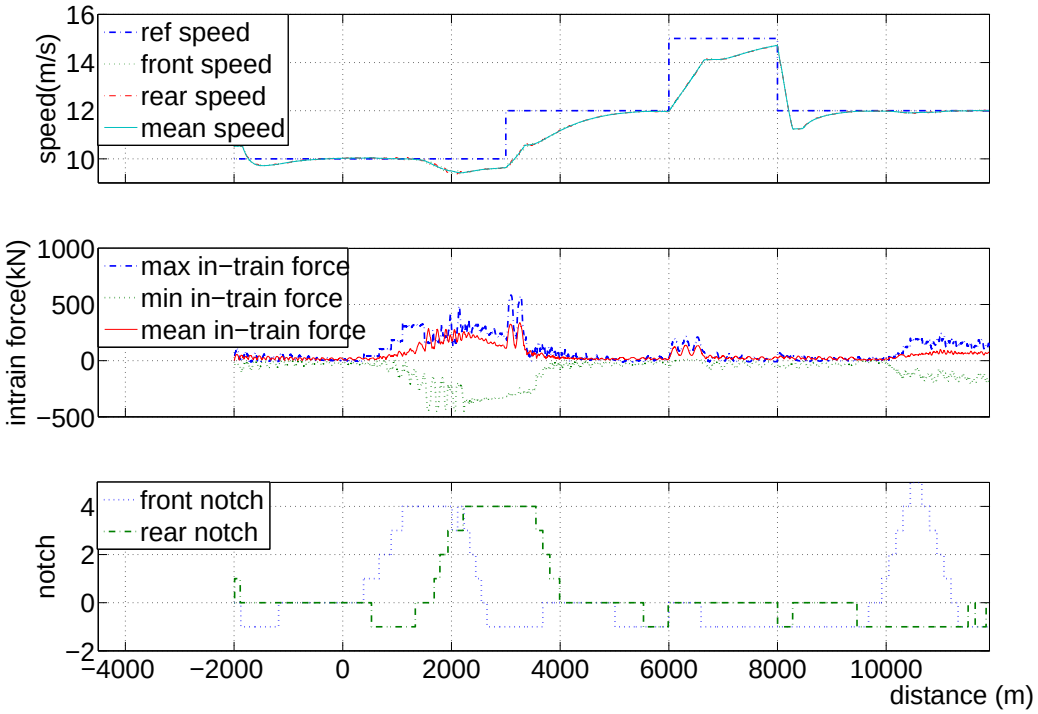

Figure 5.15: Front-loco-fault with an FTC

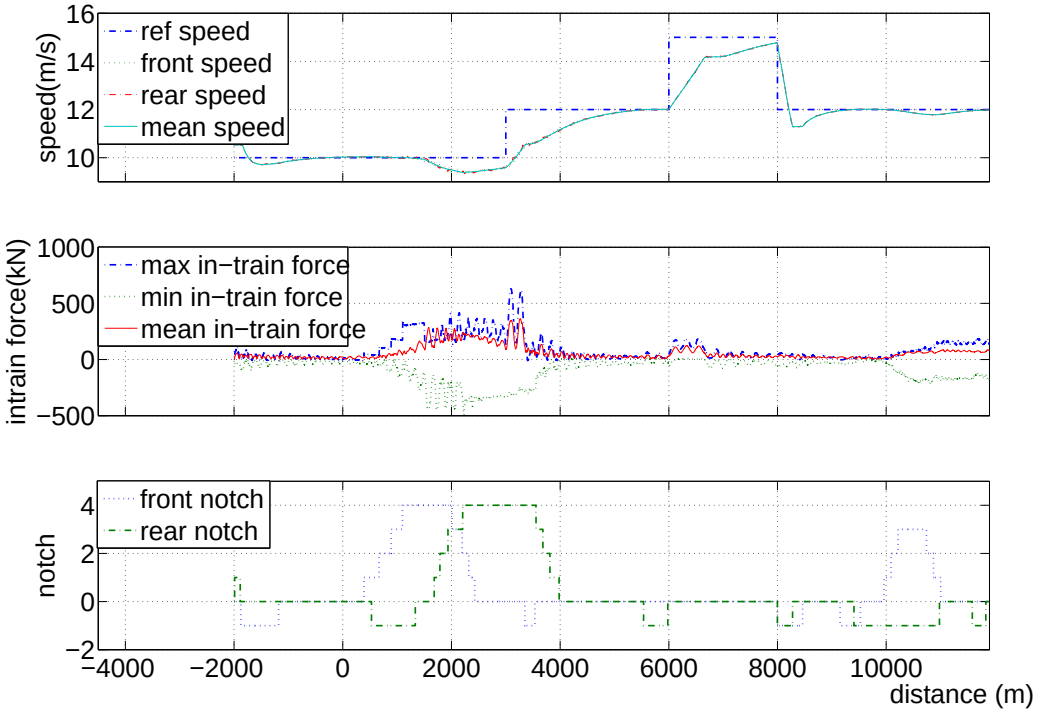

Figure 5.16: Front-loco-fault with a non-FTC

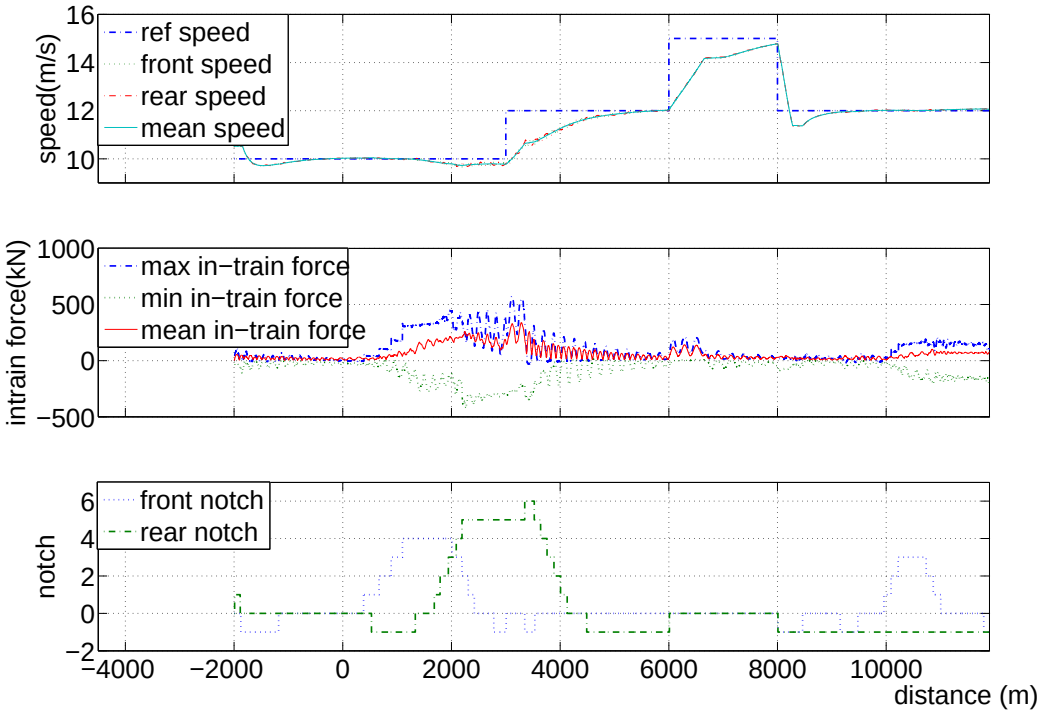

Figure 5.17: Rear-loco-fault with an FTC

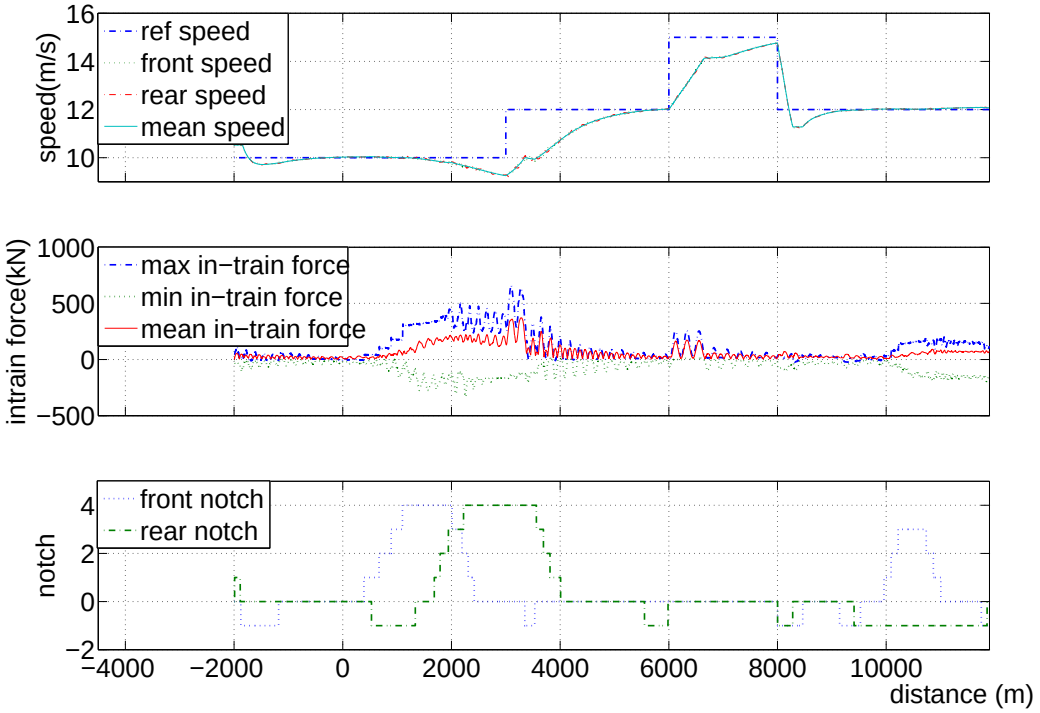

Figure 5.18: Rear-loco-fault with a non-FTC

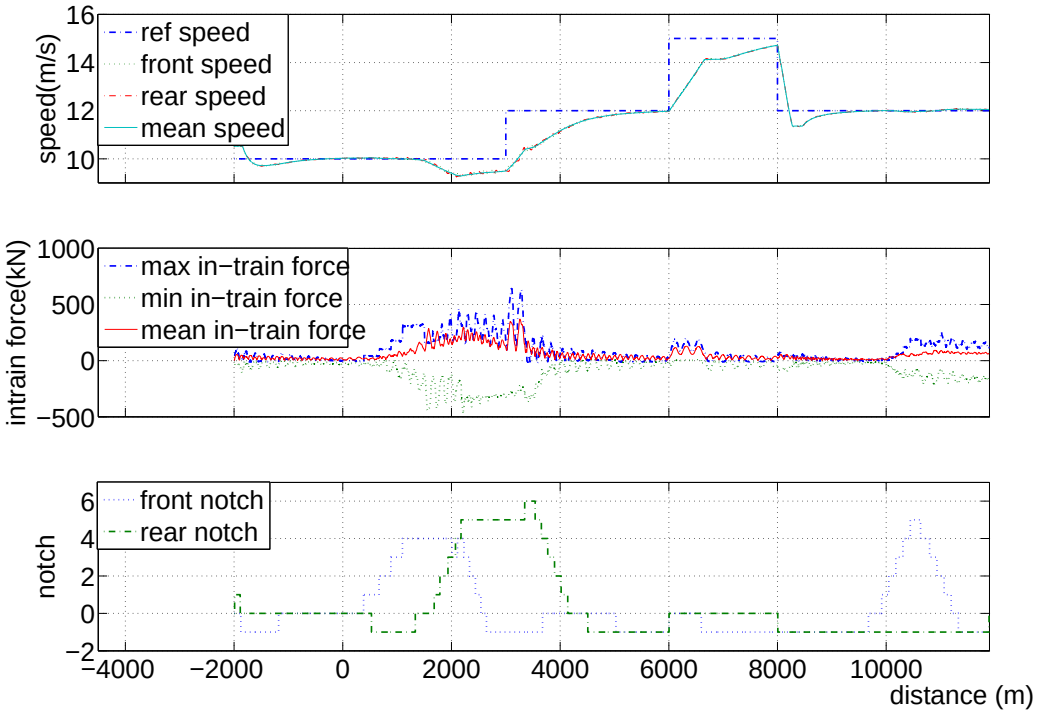

Figure 5.19: Both-loco-fault with an FTC

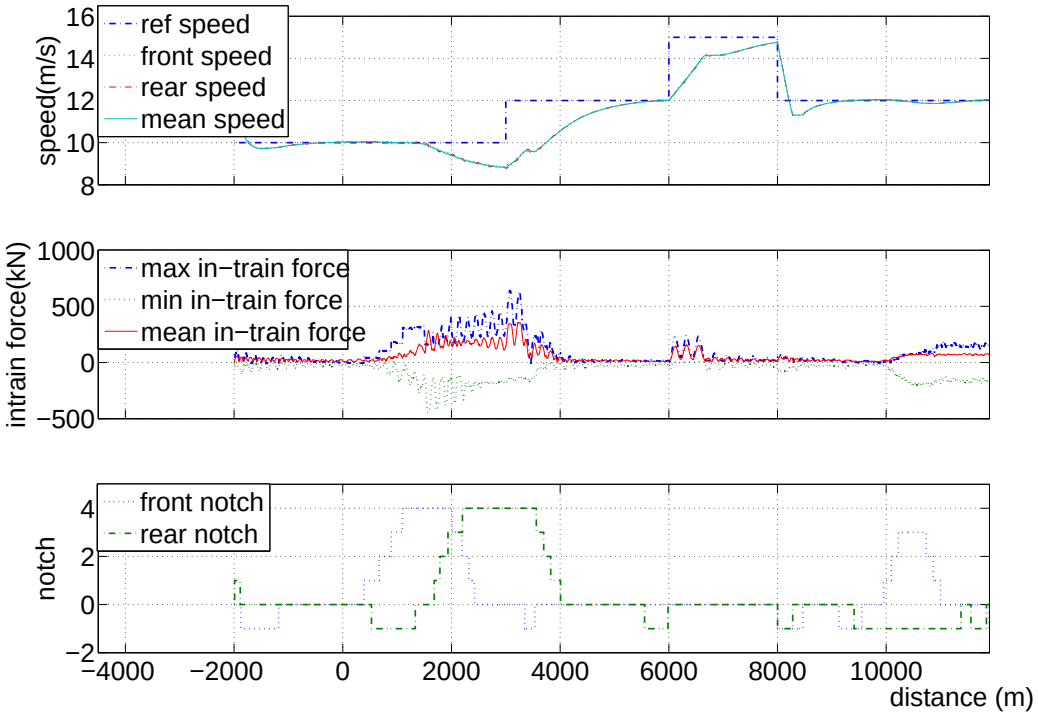

Figure 5.20: Both-loco-fault with a non-FTC

Table 5.2: Comparison of non-FTC and FTC of locomotive faults

	$\lvert\delta\bar{v}\rvert$(m/s)			$\overline{\lvert f_{in}\rvert}$(kN)			E
	max	mean	std	max	mean	std	(MJ)
Fig. 5.15	3.0302	0.4068	0.56	338.40	56.57	65.32	11,600
Fig. 5.16	2.9863	0.4061	0.55	361.80	60.19	65.19	10,800
Fig. 5.17	2.9773	0.3498	0.54	339.61	64.53	63.98	12,200
Fig. 5.18	2.9786	0.4505	0.65	372.29	64.31	65.98	9,680
Fig. 5.19	3.0244	0.4180	0.57	370.39	60.00	64.87	11,400
Fig. 5.20	3.1717	0.5349	0.73	355.97	58.80	66.31	7,800

5.6.3 Simulation of wagon faults

In previous sections, an approach of calculation of the steady-state speed difference as an FDI of the wagons' brake fault was proposed. In simulation, all faults occur from the distance $1,500$ m. The simulation results are shown below.

Fig. 5.21 depicts the simulation of an FTC of the wagon braking system with a faultless system. The corresponding simulation of a non-FTC is the same as Fig. 4.2. In comparing these two figures, one can see that the FTC does not explicitly worsen the performance of the speed regulator.

Fig. 5.22 and Fig. 5.23 represent the simulation results of an FTC and a non-FTC when the braking system makes only 97% of the expected braking efforts. This fault is very small. From a comparison of the FTC and the non-FTC, the difference between them is very small. Also from comparing Fig. 5.22 with Fig. 5.21, one knows such a small fault does not affect the performance of the speed regulator.

When a more serious fault occurs (the braking system makes 70% of the expected braking efforts), the difference between the FTC and the non-FTC is obvious, which can be seen from a comparison of Fig. 5.24 with Fig. 5.25. The former is with an FTC and the latter with a non-FTC.

When only part of the braking efforts are faulty, the performance of an FTC is also better than that of a non-FTC, although the FTC is designed for the whole braking system, which can be seen from a comparison of Fig. 5.26 with Fig. 5.27. In Fig. 5.26 and Fig. 5.27, the outputs of wagons numbered from 2 to 31 are 70% of the expected. The performance comparison is shown in Table 5.3.

From the above comparison, one can draw the following conclusions:

1) A small fault in the braking system has very little effect on the performance of the speed regulator.

2) The application of an FTC together with a speed regulator does not explicitly

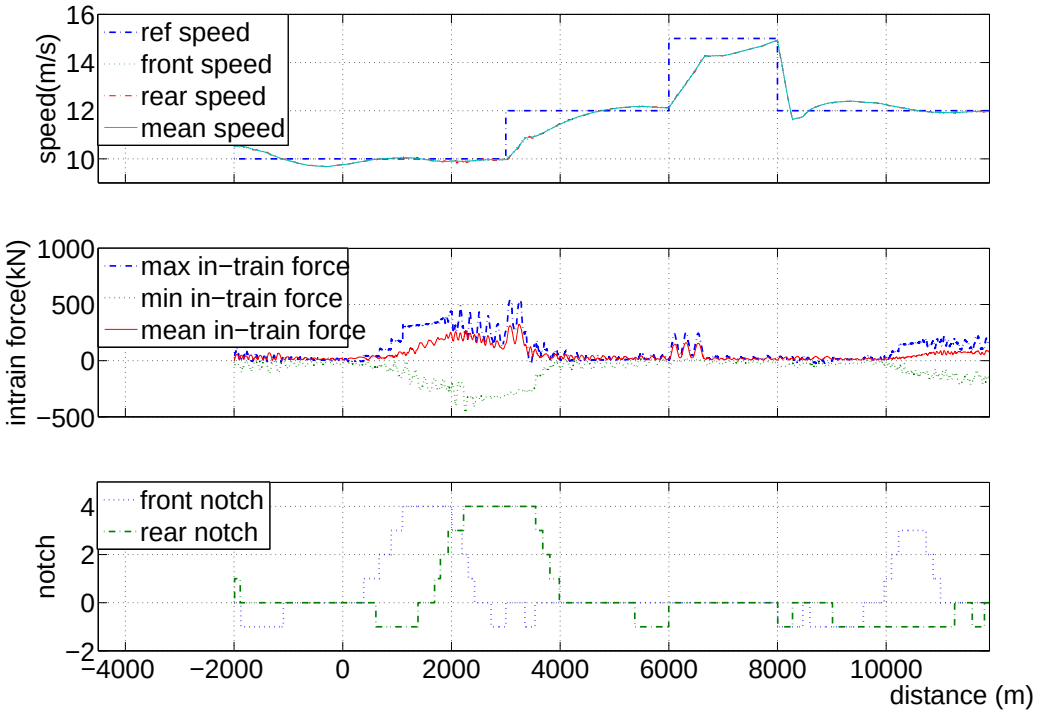

Figure 5.21: Faultless train with an FTC of braking system

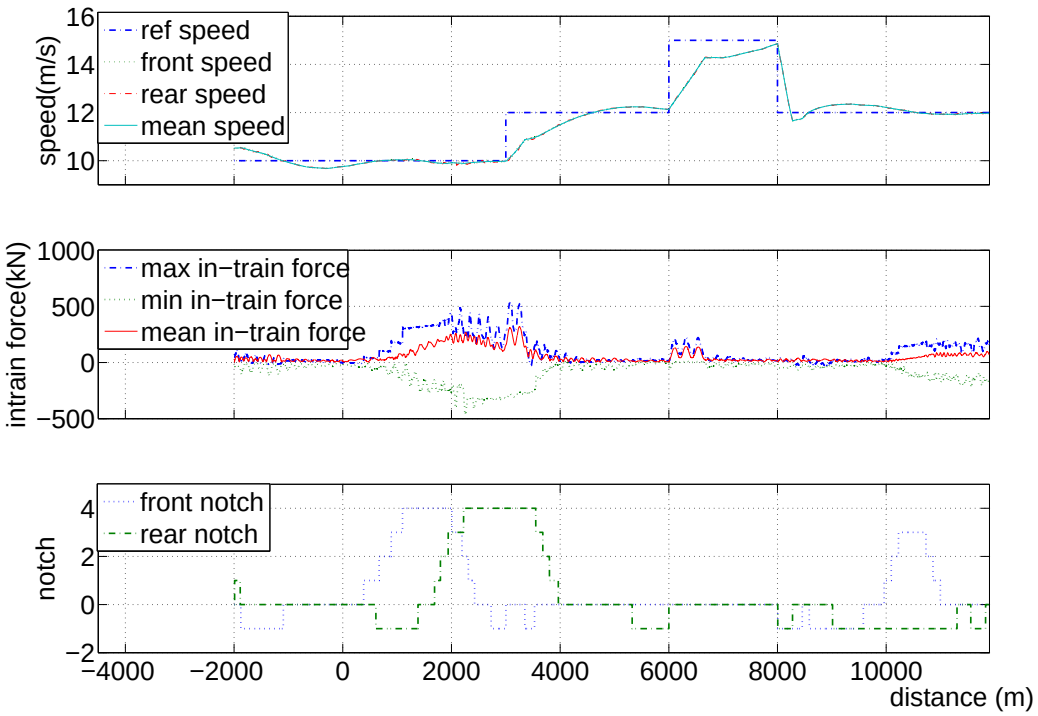

Figure 5.22: Small fault in an FTC of braking system

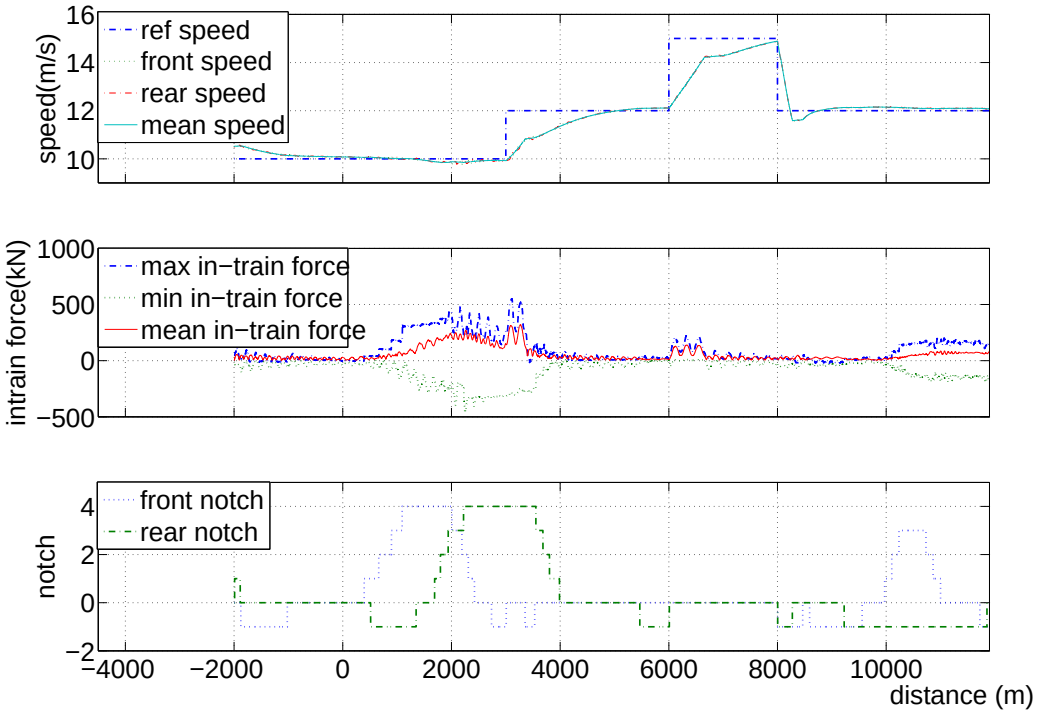

Figure 5.23: Small fault in a non-FTC

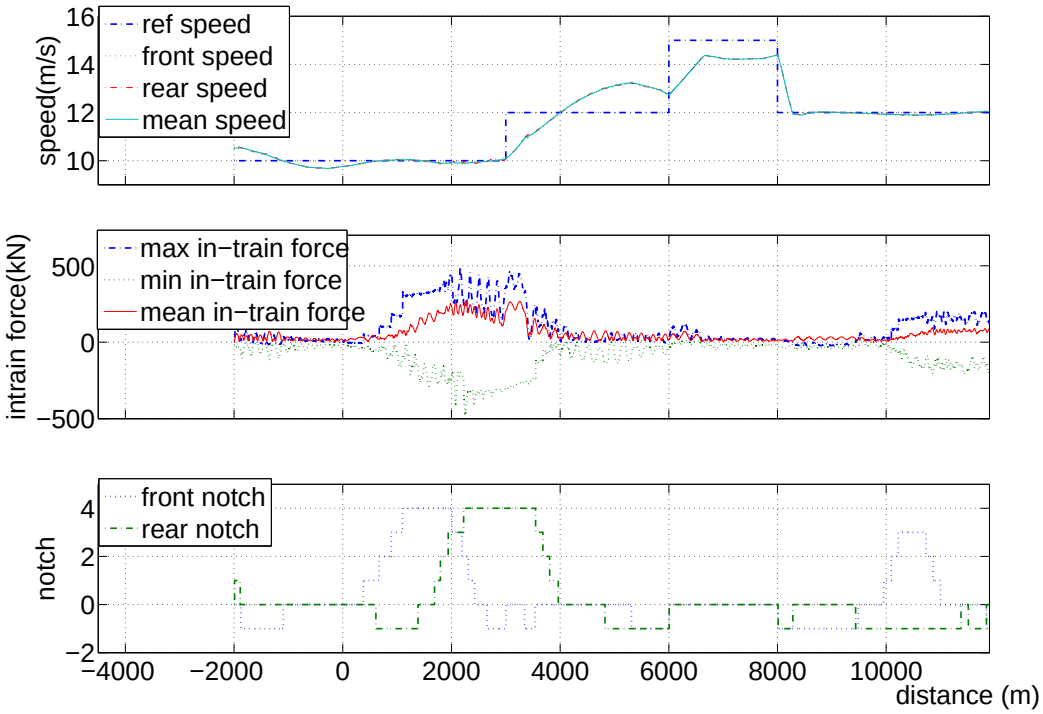

Figure 5.24: Big fault in an FTC of braking system

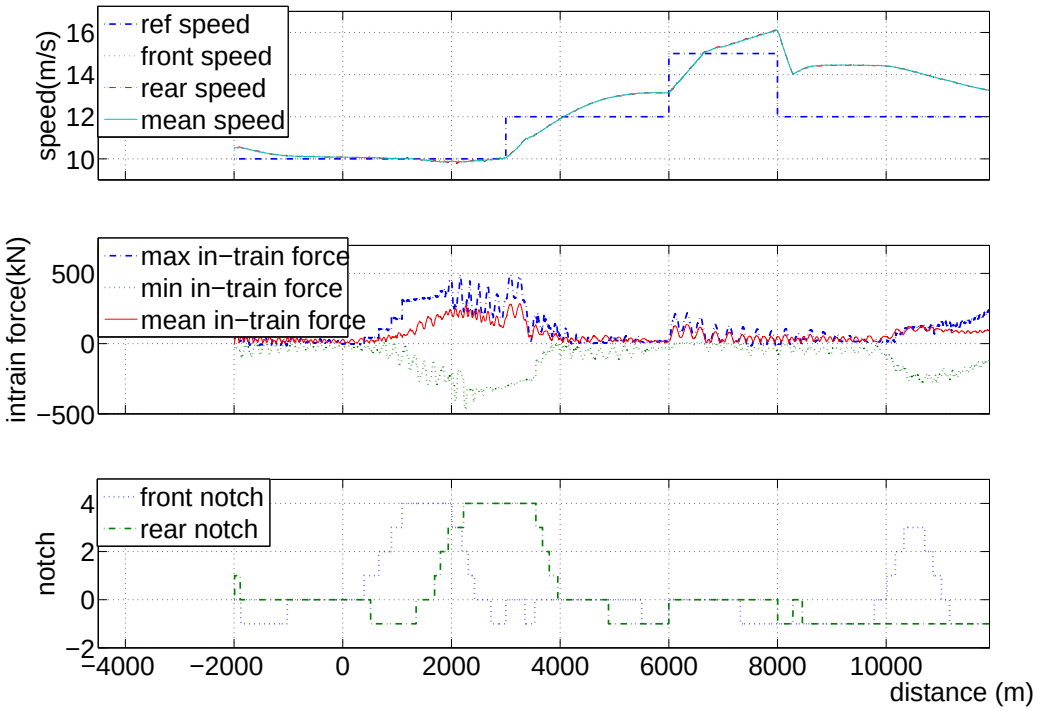

Figure 5.25: Big fault in a non-FTC

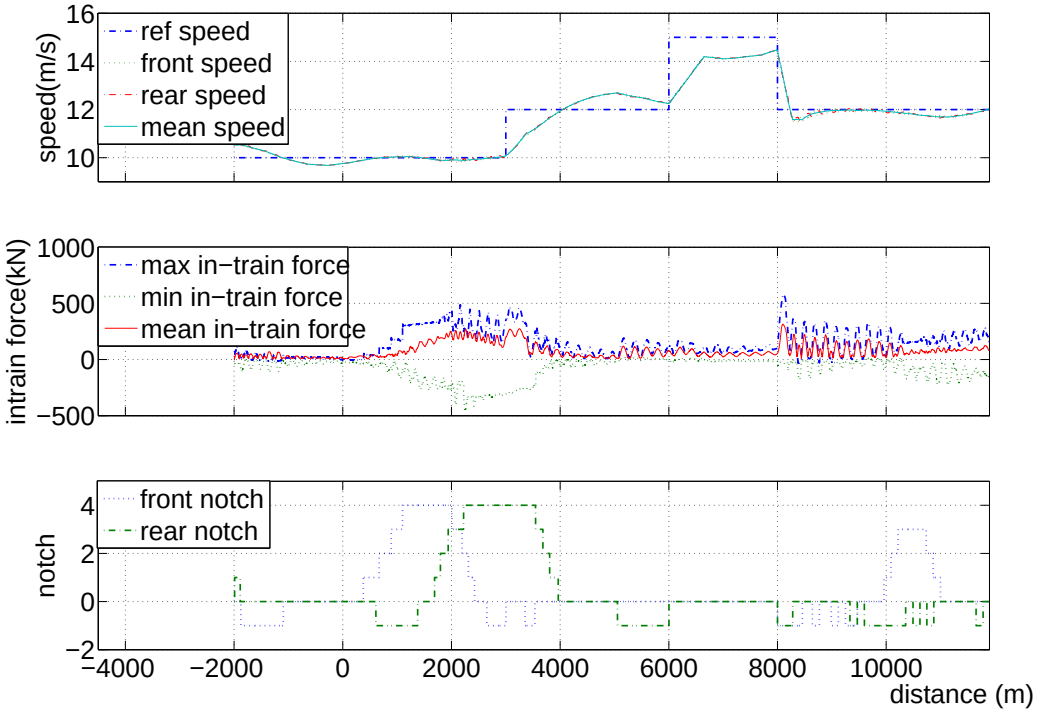

Figure 5.26: Partial fault in an FTC of braking system

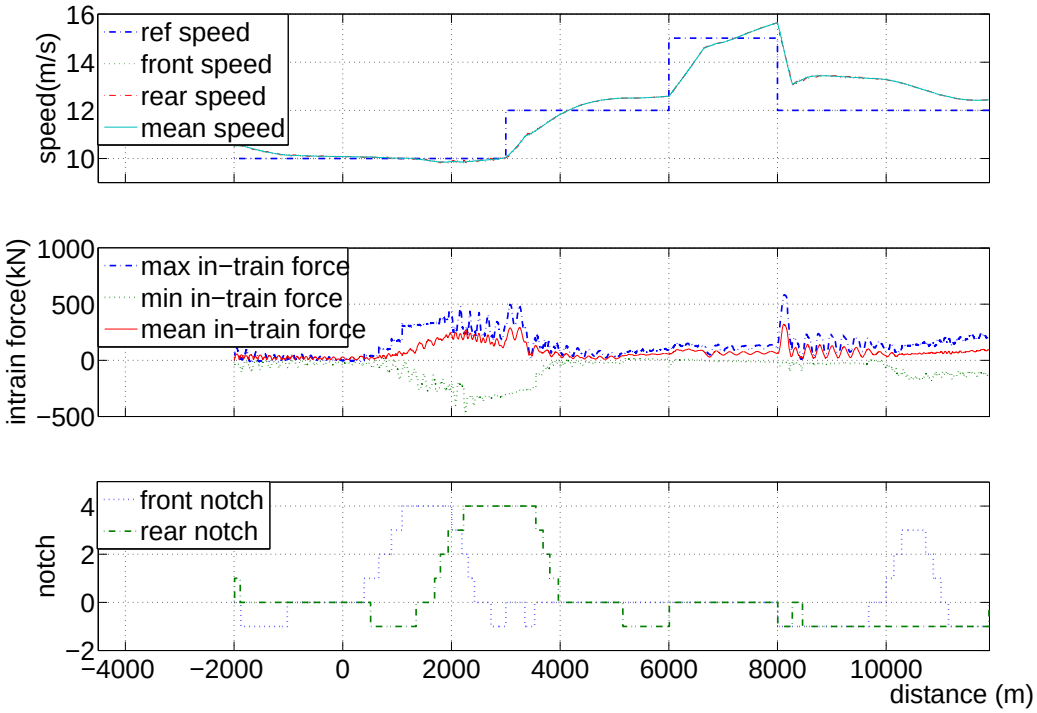

Figure 5.27: Partial fault in a non-FTC

Table 5.3: Comparison of non-FTC and FTC of wagon faults

	$\lvert\delta\bar{v}\rvert$(m/s)			$\overline{\lvert f_{in}\rvert}$(kN)			E
	max	mean	std	max	mean	std	(MJ)
Fig. 5.21	2.9227	0.3480	0.49	323.89	56.64	63.99	12,300
Fig. 4.2	2.9863	0.4061	0.55	361.80	60.19	65.19	10,800
Fig. 5.22	2.8723	0.3458	0.48	321.31	55.86	63.70	12,300
Fig. 5.23	2.8913	0.3299	0.50	321.64	56.79	63.51	12,299
Fig. 5.26	2.7629	0.3728	0.47	315.71	78.30	66.15	12,256
Fig. 5.27	3.6407	0.5251	0.56	322.02	75.93	63.79	11,957

worsen the performance of the speed regulator when the system is faultless.

3) When a small fault occurs, there is little difference between the application of an FTC and a non-FTC.

4) The application of an FTC can improve the performance when a big fault of the braking system occurs.

5) Even if a fault occurs in part of the braking system, which is different from the assumed fault in (5.25) (fault with the whole braking system), the application of an FTC can improve the performance of the speed regulator.

5.7 Conclusion

In this chapter, the fault-tolerant control of the handling of heavy haul trains is discussed. The discussion is based on the redesign of the speed regulator with measurements proposed in chapter 4.

The FDIs for the gain faults of the sensors and the braking system are respectively studied, while the FDI of the locomotive fault is not studied in this thesis, but can be done following some other approaches, such as one proposed in [69]. The FDI of sensor faults is based on a geometric approach proposed in [61]. The FDI of a braking system is based on observation of the steady-state speed. From the difference of the steady speed between the fault system and the faultless system, one can get the fault information.

These two kinds of FDIs are studied separately, but need to be studied further together. In the opinion of the researcher, it is possible to apply them together, because the FDI of a sensor fault is based on the difference between the measured speed of a sensor and the estimated speed of the observer while the FDI of a braking fault is based on the difference between the measured speeds (steady-state speeds) and the reference speed. In the former, a necessary condition for the diagnosis of a fault is that there are differences among the measured speeds while in the latter, a necessary condition for a diagnosis of a fault is that there are nearly no differences among the measured speeds (because a steady state is assumed). This is, however, just a theoretical discussion. In fact, because of the accuracy of the sensor and the ideal assumption of a steady state, the judgement of the difference among the measured speeds depends on a threshold. This is a difficult problem. The setting of a threshold affects the performance of the two FDIs, which is not discussed in this chapter.

In simulation, tests were conducted on the suitability of the two FDIs and the redesign of speed regulators according to the fault signals from the FDIs of sensor faults and braking system faults, and the FDI (not included in this study) of locomotive faults.

Simulation shows that the random errors of the speed sensors have very little impact on the train's performance. It is also shown that the proposed fault-tolerant controller does not explicitly worsen the performance of the speed regulator in the case of a faultless system, while it obviously improves the performance of the speed regulator in the case of a faulty system. It should be pointed out that the approach in this chapter cannot guarantee performance in the case of the occurrence of a serious fault.